

Marta Clelia Ruch

Applied Research Division  
Structural and Nondestructive Testing Department (ENDE)  
Argentine Atomic Energy Commission  
(Comision Nacional de Energia Atomica, CNEA)

Centro Atomico Constituyentes  
Av. General Paz 1499, 1650 San Martin,  
Provincia de Buenos Aires, Argentina  
Phone: +(54) 11 6772 7739  
Fax: +(54) 11 6772 7233  
E-mail: [ruch@cnea.gov.ar](mailto:ruch@cnea.gov.ar)



## Introduction

Material characterization

Basic work:

Corrosion of Zr-base alloys

Eddy currents testing: probe design

Modelling

Steels

Evaluation of damage

Review of literature on Zr hydrides

International projects:

IAEA – CRP

NIRDTP

IZFP

# Career profile

Research in electromagnetic methods of nondestructive evaluation; eddy current testing; material characterization; corrosion; phase transformations; X-ray diffraction; nuclear energy.

1976: University Diploma in Physics (Licenciada en Ciencias Físicas) from the University of Buenos Aires.

Graduate thesis: “Microanalysis with the laser microprobe LMA1 – Karl Zeiss – Jena”

1976: Advanced Training Course on Metallurgy – OEA - CNEA

1989: Ph D in Physics (Doctora en Ciencias Físicas) from the University of Buenos Aires.

Doctoral thesis: “Ti, Zr and the Ti-Zr system: phase diagrams and associated transformations”

1996: Level 3 Certificate, Eddy currents testing, IRAM-ISO 9712, periodically renewed and recertified. Last recertification: April 2016.

I entered the NDT Department (INEND, created in 1976) in its early stages, where I was trained in different methods of NDT, mainly eddy current testing (ET) and ultrasound (UT), took level 2 courses and worked in R/D in various aspects of both methods, until I finally devoted myself to ET. In parallel, I was preparing my PhD dissertation at the Materials Department.

By 1988, as Head of the Applied Research Group, I started fostering R/D and inspection activities in ET, as well as in Acoustic Emission and Optics.

My background as a metallurgist led me to work in multidisciplinary groups devoted to the follow-up of components of nuclear power plants (NPP's) and to material characterization / degradation, always contributing the NDT point of view. The materials of interest are mainly Zr and its alloys (so-called nuclear materials: fuel cladding, fuel channels, pressure tubes), steels, nickel alloys (incolloys used in steam generators of NPP), aluminium.

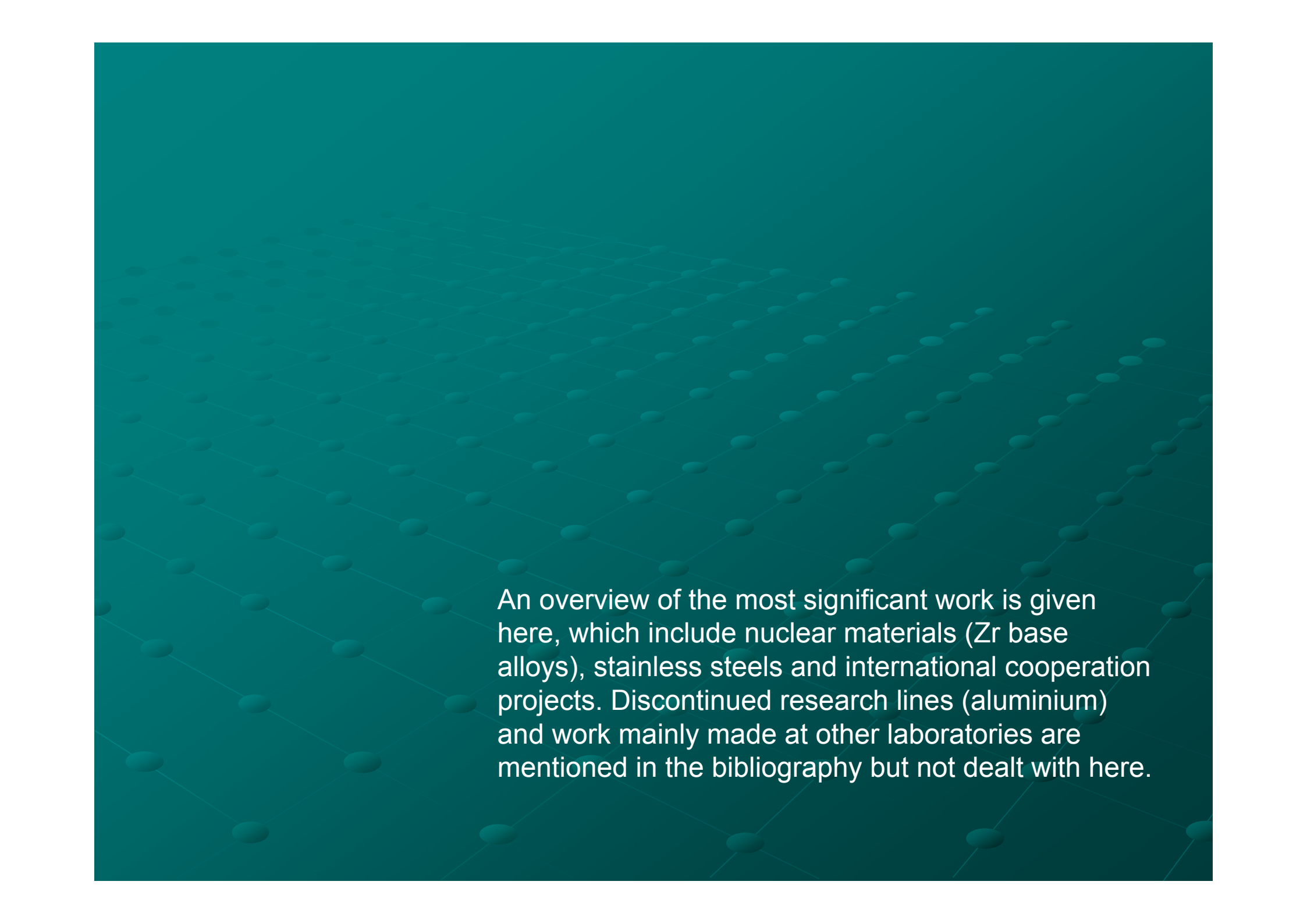
In 1994 I was appointed member of the first examination – certification board on ET and received in 1996 my IRAM-ISO 9712 Level 3 ET Certificate, pioneering the certification in that method in Argentina.

I participate in several international cooperation projects, within the framework of which I visited sister-institutions abroad.

# Areas of interest

- Nondestructive evaluation
- Eddy currents
- Probe design
- Modelling
- Magnetic measurements
- Corrosion
- Hydriding
- Phase transformations
- Materials:
- Zirconium base alloys.
- Aluminium
- Stainless steels
- Ceramics
- Coatings

The work normally consists in the preparation of test specimens by autoclave or thermomechanical treatments and their characterization using different techniques, metallography, XRD, electromagnetic nondestructive techniques. In some cases, special techniques were adapted or developed.



An overview of the most significant work is given here, which include nuclear materials (Zr base alloys), stainless steels and international cooperation projects. Discontinued research lines (aluminium) and work mainly made at other laboratories are mentioned in the bibliography but not dealt with here.

Introduction

Material characterization

Basic work:

Corrosion of Zr-base alloys

Eddy currents testing: probe design

Modelling

Steels

Evaluation of damage

Review of literature on Zr hydrides

International projects:

IAEA – CRP

NIRDTP

IZFP



# Study of Zircaloy-4 corroded in autoclave for its NDT characterization with planar coils eddy current testing

**PhD student:** Mag. Lic. Javier Fava

**Counsellors:** Dra. Marta Ruch  
Dra. Liliana Lanzani

ENDE and Material Departments. Centro Atómico Constituyentes. CNEA.

# Corrosion of Zr-base alloys

- Autoclave corrosion in 1M LiOH at 340°C and equilibrium pressure 13.6 MPa
- $\text{Zr} + 2\text{H}_2\text{O} \rightarrow \text{ZrO}_2 + 2\text{H}_2$
- $\text{H}_2$  diffuses into the material
- Conditions are similar to in-pile corrosion, but accelerated and there is no radiation.
- An oxide layer grows on the surface.
- $\text{H}_2$  liberated by the corrosion reaction enters the alloy, a hydride layer growing below the surface.
- Heat treatments for the homogeneization of H and Zr-hydrides in the bulk are necessary.

# Corrosion of Zr-base alloys

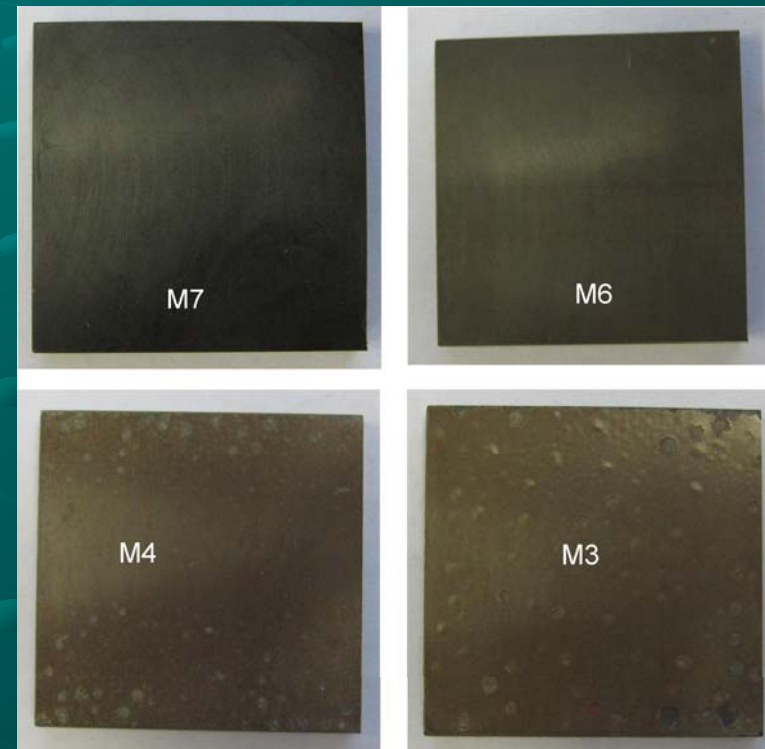
## Autoclave treatment

- Specimens were studied by weight gain, metallography, X-ray diffraction, optical and electronic microscopy, eddy currents.  
Planar and pancake coils were used.  
A model for impedance  $Z$  and parameter extraction was developed.
- Micrographs of the specimens, showing oxide layers and hydride distribution are presented.
- Results are summarized in a table.

# Autoclave treatment of Zircaloy-4 in 1M LiOH at 340°C and equilibrium pressure 13.6 MPa

Top view of oxidized  
Zircaloy-4 thick specimens  
(4 mm thick)

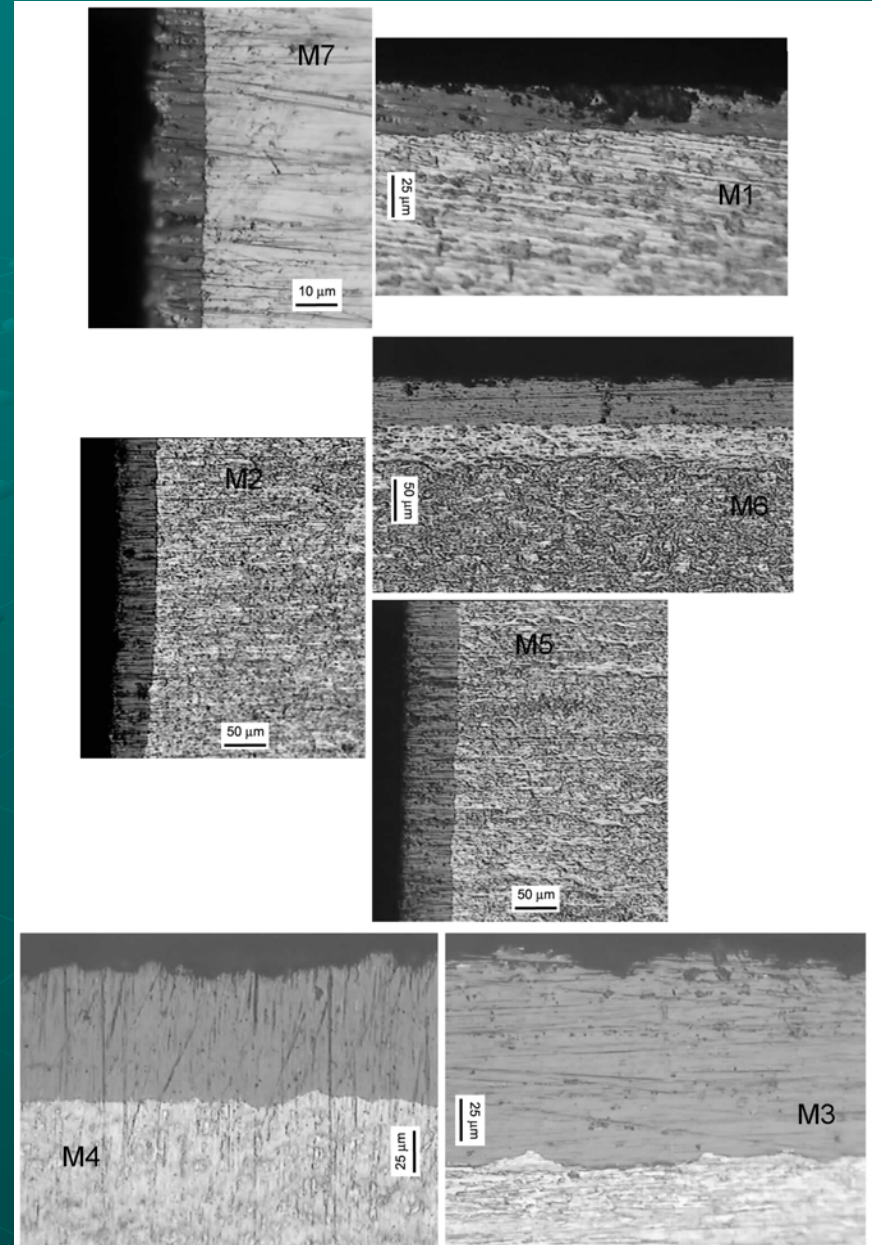
	M7	M1	M2	M6	M5	M4	M3
Specific weight gain [mg/dm <sup>2</sup> ]	233	416	683	1018	1392	1658	2496
Oxide thickness [μm]	17	30	53	75	103	106	172
Hydrogen [wt ppm]	142	231	687	835	1204	1296	2019



Autoclave treatment  
of Zircaloy-4 in 1M  
LiOH at 340°C and  
equilibrium pressure  
13.6 MPa

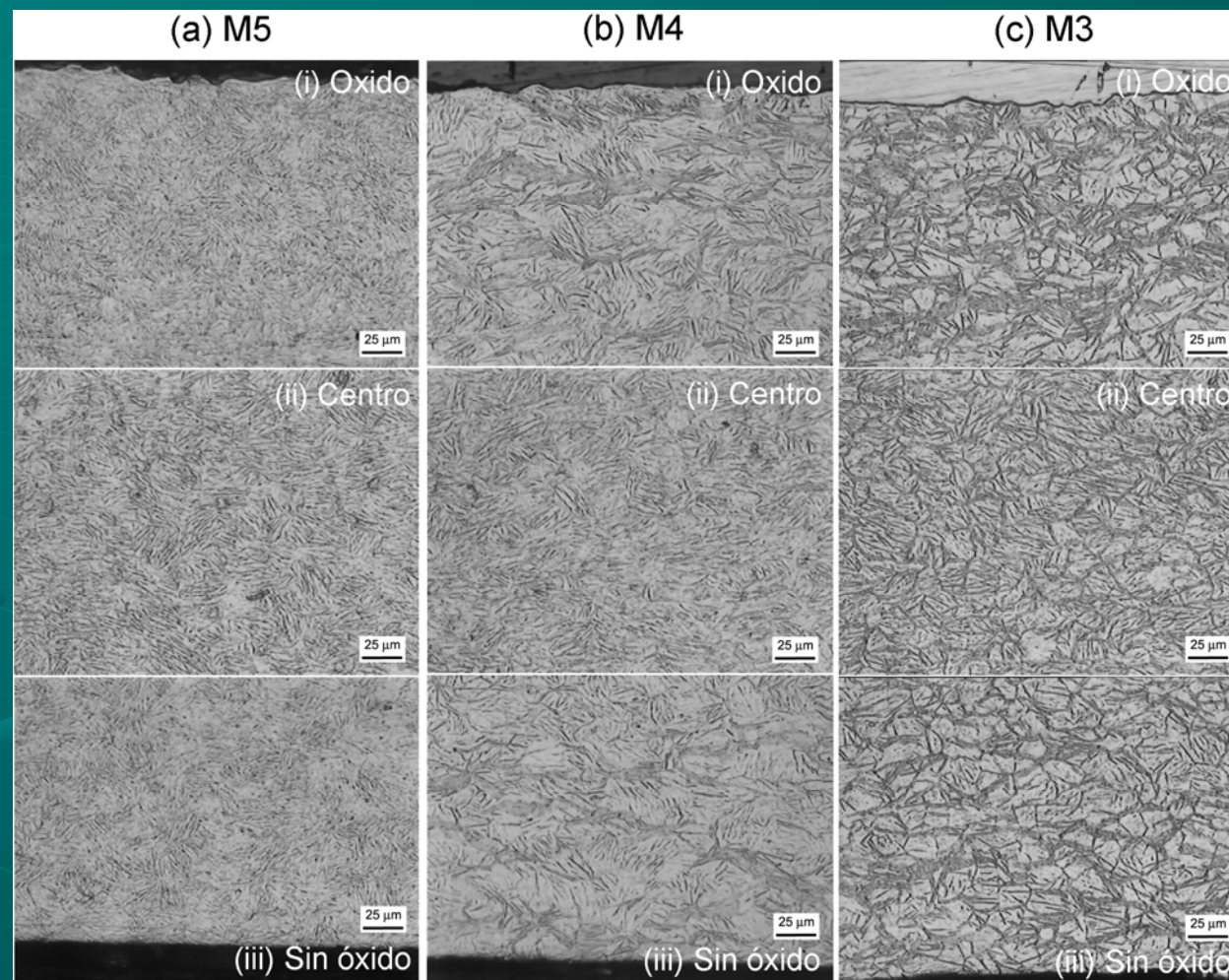
Cross section of the  
autoclave grown oxides on  
the Zry-4 specimens.

Optical microscopy



Autoclave  
treatment of  
Zircaloy-4 in 1M  
LiOH at 340°C  
and equilibrium  
pressure 13.6  
MPa

Delta-hydrides in some specimens



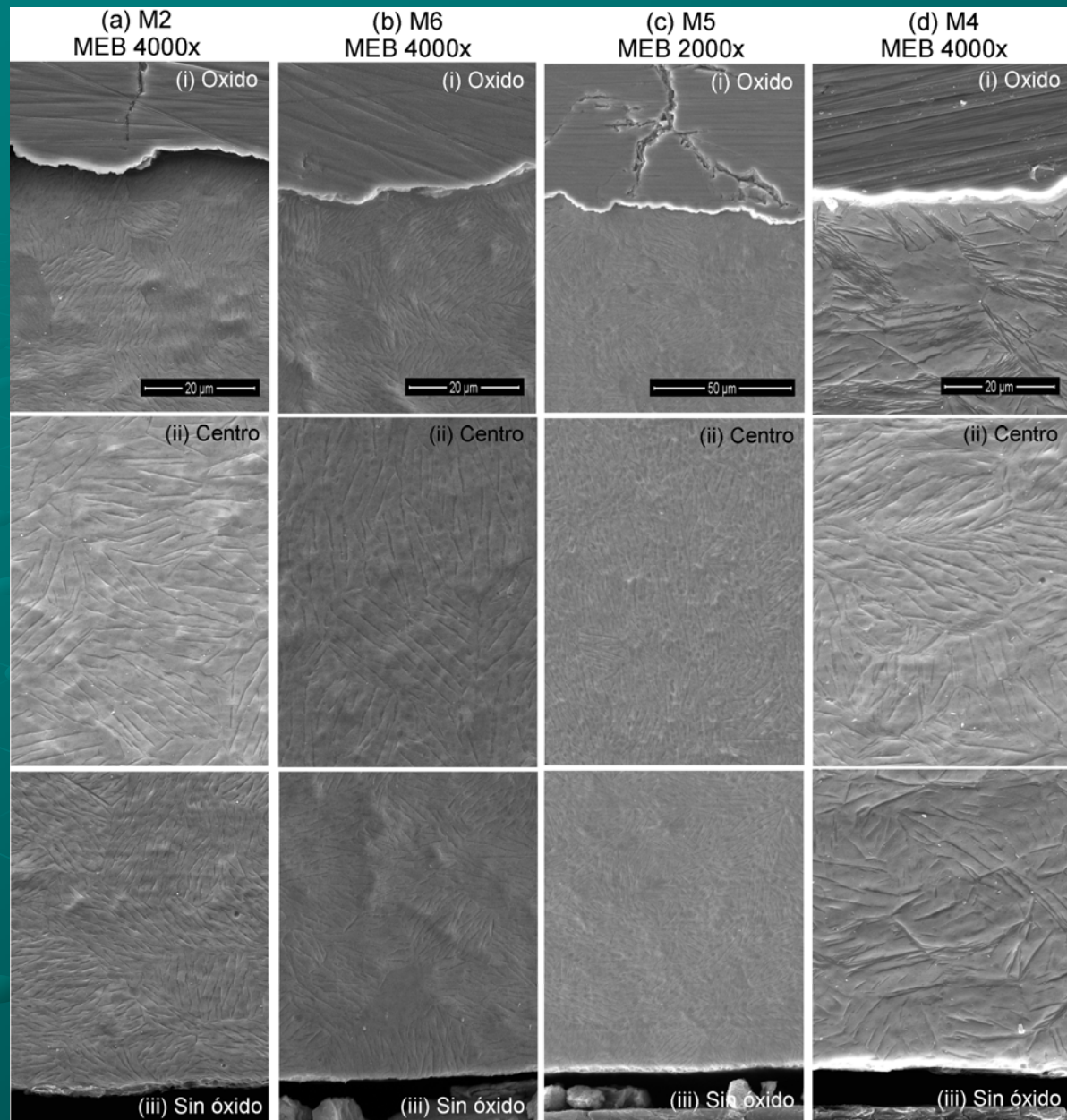
1204 ppm H

1296 ppm H

2019 ppm H

Autoclave  
treatment of  
Zircaloy-4 in 1M  
LiOH at 340°C  
and equilibrium  
pressure 13.6  
MPa

Electron  
microscopy



687 ppm H

835 ppm H

1204 ppm H

1296 ppm H

Introduction

Material characterization

Basic work:

Corrosion of Zr-base alloys

Steels

Eddy currents testing: probe design

Modelling

Evaluation of damage

International projects:

IAEA – CRP

NIRDTP

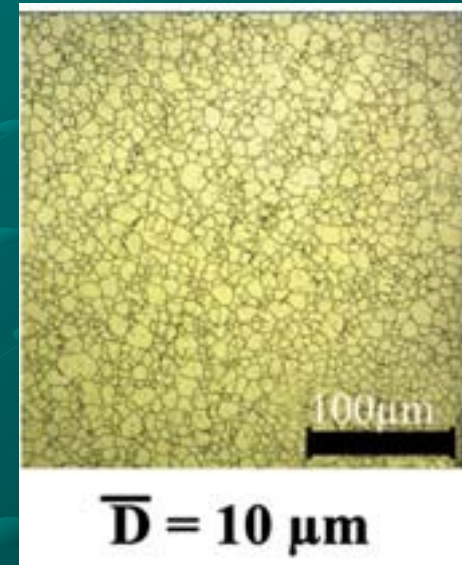
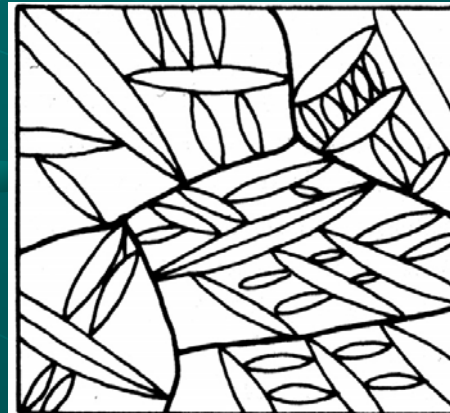
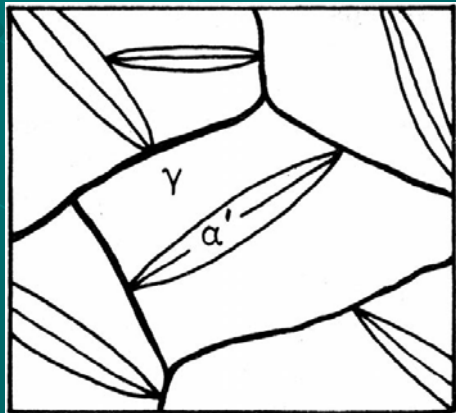
IZFP

# Metastable austenitic steels

In steels,  $\gamma$  to  $\alpha$  transformation takes place on cooling, the amount and morphology of the low temperature phases depending on composition, cooling rate, strain-stress conditions, etc

Austenitic stainless steels: retain the  $\gamma$  phase down to room temperature (RT) ( $M_s$  is very low)

in Austenitic SS, deformation induced martensite (DIM) can be formed at  $T < M_d (> M_s)$



Equilibrium austenite. From Shirdel et al. Mat. Charact 103(2015) 150-161

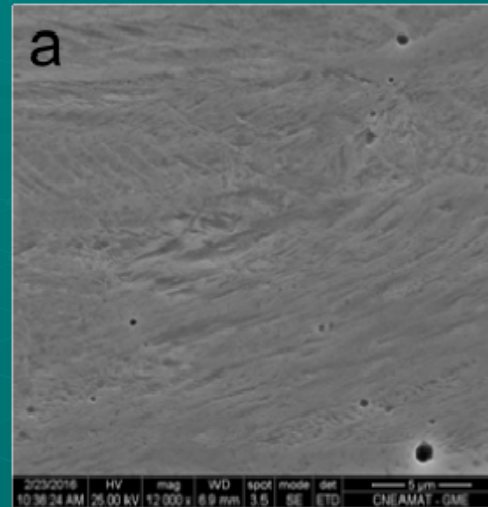
# Reversion of martensite

- Specimens of AISI-304 and 316 stainless steels available at the lab were re-examined to study the reversion of martensite in metastable austenitic steels.
- Metallography, eddy currents and magnetic techniques were used to study the evolution of reversion as a function of temperature of heat treatment (HT). All studies were made at room temperature.
- New interest in this material prompted by its fine grained structure with enhanced hardness and good corrosion resistance properties.

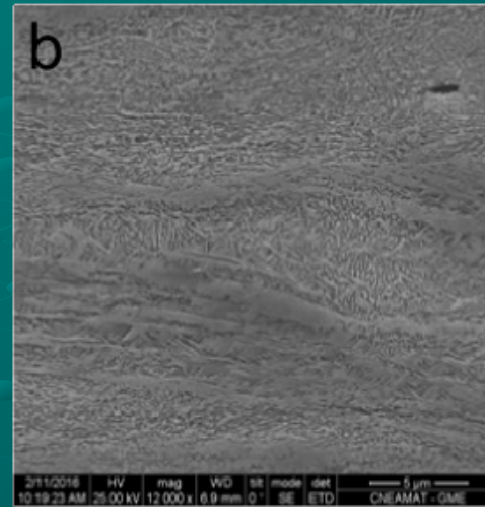
# Reversion of $\alpha'$ Martensite

SEM images of HT-specimens AISI 304 steel 12000X.

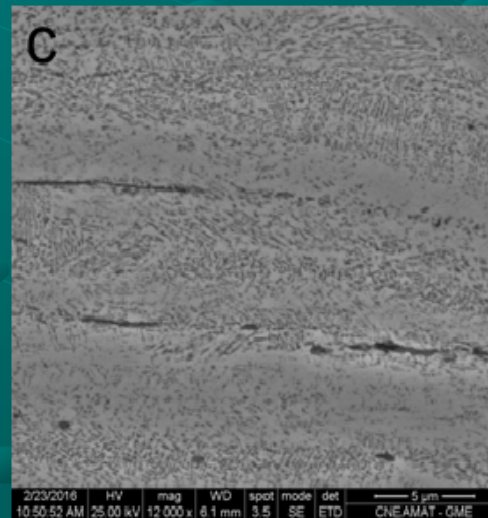
a) 4-yz (550°C);  
needle-like martensite



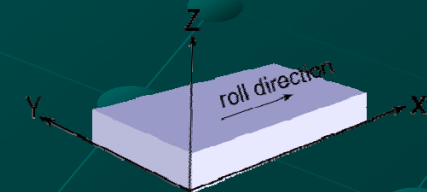
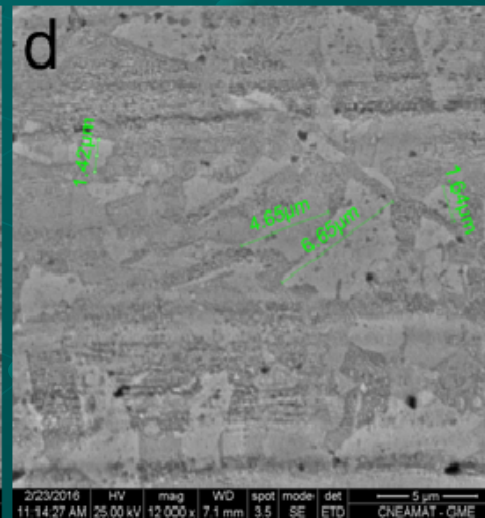
b) 7-xz (650°C); lath  
martensite  
deformation bands  
and elongated  
austenite grains in the  
rolling direction



c) 9-yz (700°C); lath  
martensite,  
deformation bands and  
elongated austenite  
grains



d) 11-xz (800°C);  
recrystallized  
austenite grains in  
a matrix of  
deformed  $\gamma$  or  $\gamma'$ .



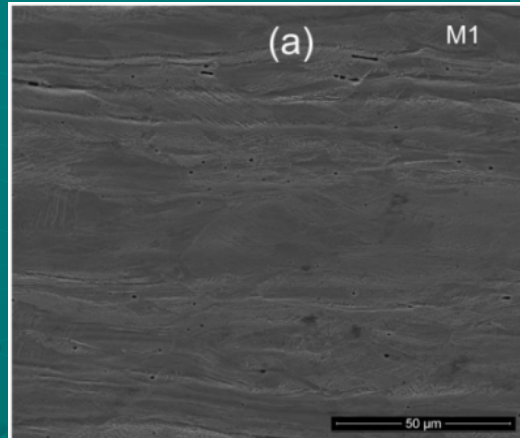
# Reversion of $\alpha'$ Martensite Microstructure

- The microstructure of the 304 specimens evolves from needle (4-yz) to lath martensite, deformation bands and elongated austenite grains following the rolling direction (7-xz), more visible in (9-yz) to recrystallized austenite grains in a matrix of deformed  $\gamma$  or  $\gamma'$  (11-xz)
- All the 316 specimens have austenite grains elongated in the rolling direction, which indicate that the texture in the material is conserved even after the high temperature HT. Two types of microstructures are observed. In specimens up to M6 (700°C),  $\alpha'$  lath martensite is observed, even after an increase in the amount of reversed austenite  $\gamma'$  for higher temperatures. The microstructure of  $\gamma'$  is very similar to that of  $\alpha'$

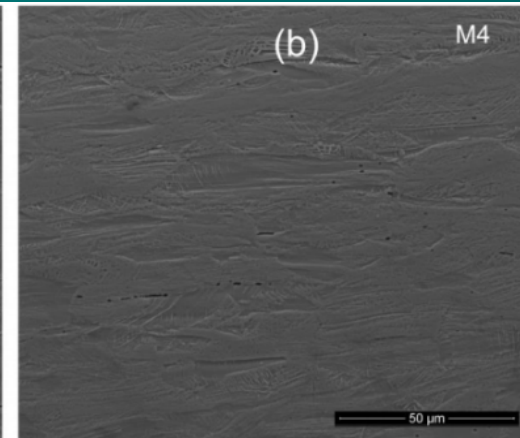
# Reversion of $\alpha'$ Martensite

SEM images of HT-specimens AISI 316 steel 1200X.

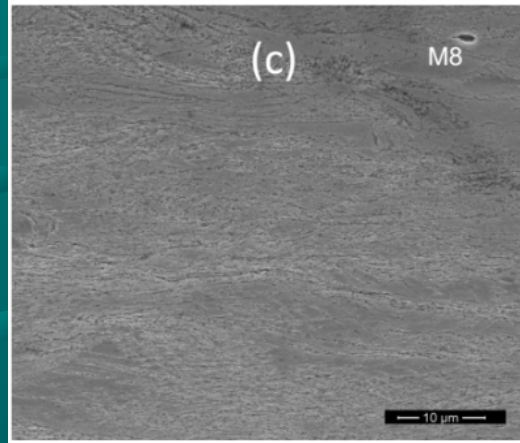
a) M1: 200° C  
33%  $\alpha'$



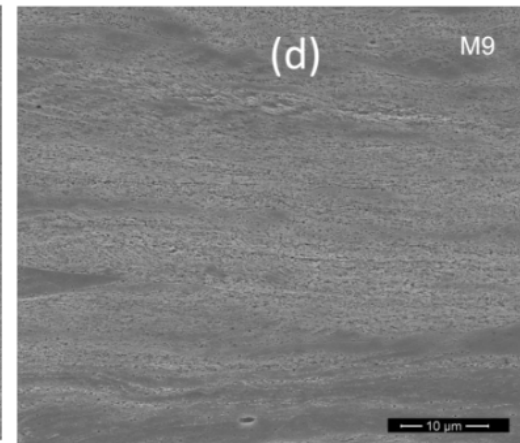
b) M4: 500° C,  
18%  $\alpha'$



c) M8:  
860° C,  
1.8%  $\alpha'$



d) M9:  
900° C,  
1.5%  $\alpha'$



Cuts: (a) and (b) cross section perpendicular to the rolling direction; (c) and (d) rolled face.

Introduction

Material characterization

Basic work:

Corrosion of Zr-base alloys

Steels

Eddy currents testing: probe design

Modelling

Evaluation of damage

Review of literature on Zr hydrides

International projects:

IAEA – CRP

NIRDTP

IZFP

# Eddy currents testing: probe design Modelling

Eddy currents are used for material characterization

Planar coils were designed and constructed.

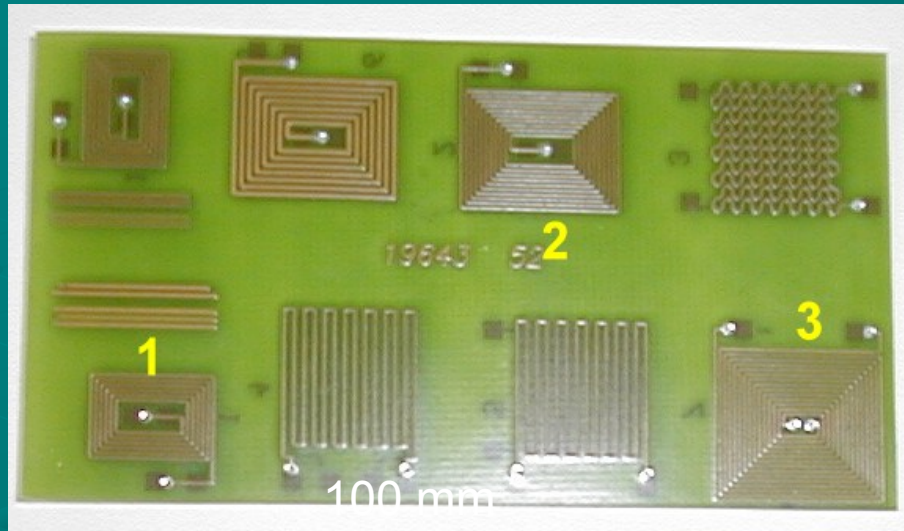
A model for coil impedance and extraction of material parameters was developed. The model follows the SOVP (Second Order Vector Potential) approach developed by Theodulidis

A quick overview of the model is given here – planar coil on planar conductive medium.

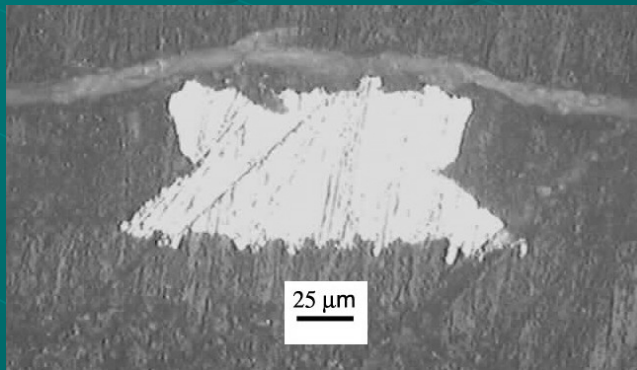
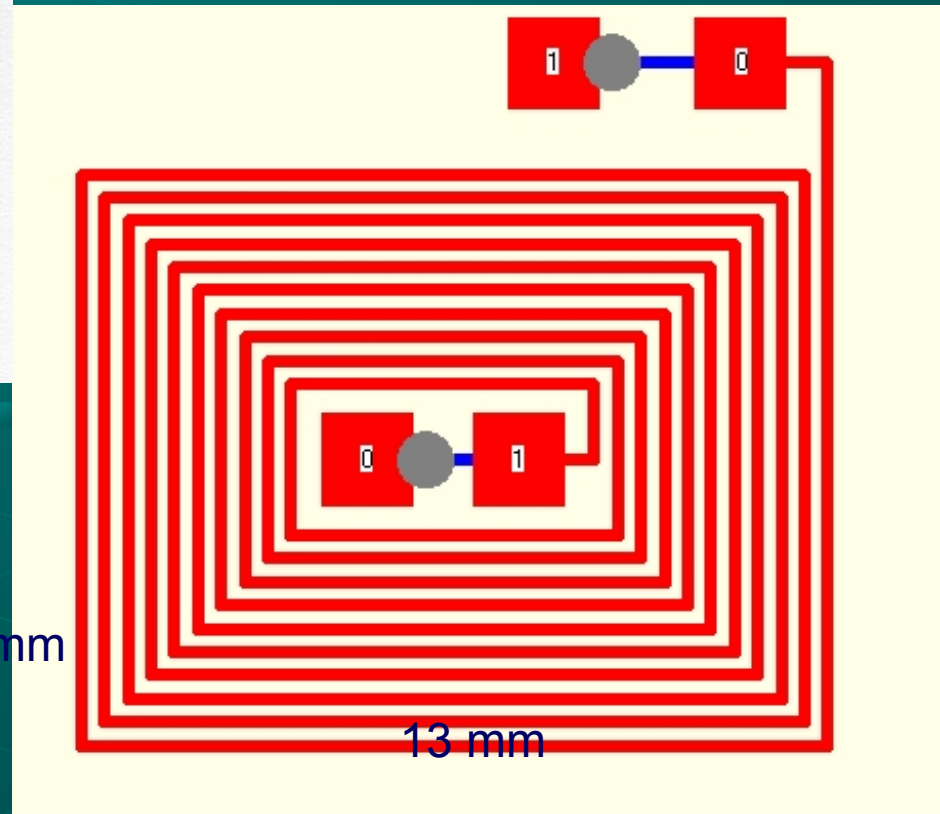
Later, planar and pancake coils were used for the inspection of the autoclave-treated Zry-4 specimens.

An 1260 Impedance Analyzer by Solartron was used for the experiments.

# Planar coils



50 mm



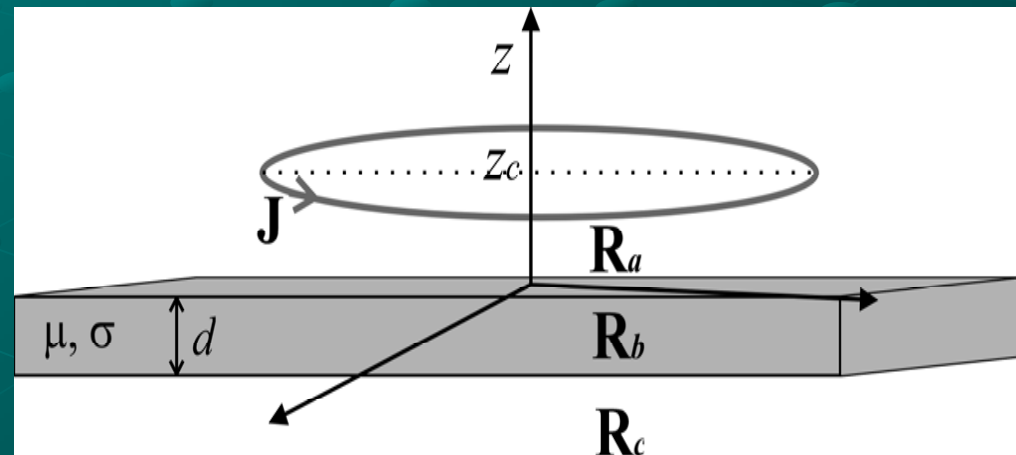
# The values to calculate

- ❖ Inductance in air ( $L_0$ )
- ❖ Impedance diagrams ( $\Delta Z$ )
- ❖ Eddy current distribution ( $J$ )

$$Z_0 = j\omega L_0$$

$$\Delta Z = \Delta R + j \Delta X$$

$$J = -j\omega\sigma A$$



$$J_c(x, t) = J_0(x)e^{j\omega t},$$

$$\omega = 2\pi f.$$

$$\mu = \mu_0\mu_r$$



# The model

**Second order vector potential approach.**

**Quasi stationary approximation.**

**Coulomb gauge,  $(\nabla \cdot \mathbf{A} = 0)$ ,  $\mu = \mu_0 \mu_r$**

$$\mathbf{A} = \nabla \times \mathbf{W}$$

$$\mathbf{W}_{a,b,c} = \hat{\mathbf{z}} W_{1,a,b,c} + \hat{\mathbf{z}} \times \nabla \cdot W_{2,a,b,c}$$

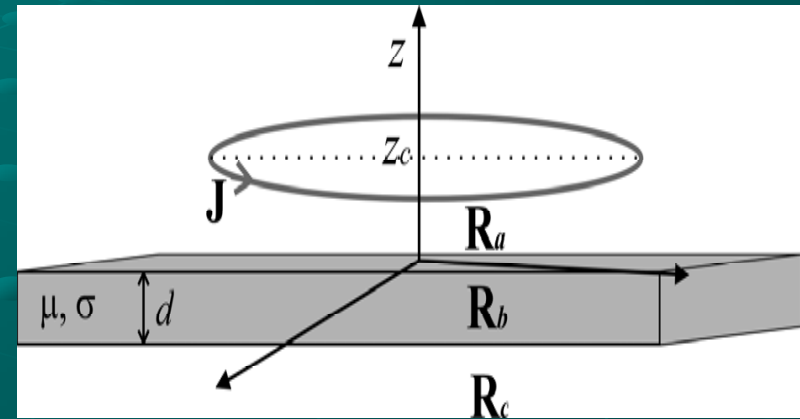
$$W_{1a} = W_{1ap} + W_{1as}$$

$$\nabla^2 \mathbf{A}_{a,b,c} - \mu \varepsilon \frac{\partial^2 \mathbf{A}_{a,b,c}}{\partial t^2} = -\mu \mathbf{J}_{a,b,c}$$

$$\nabla^2 \mathbf{A}_{a,c} = 0 \quad \text{and} \quad \mathbf{B}_{a,c} = \nabla \left( \frac{\partial W_{1a,c}}{\partial z} \right) \quad \text{in regions } R_{a,c}$$

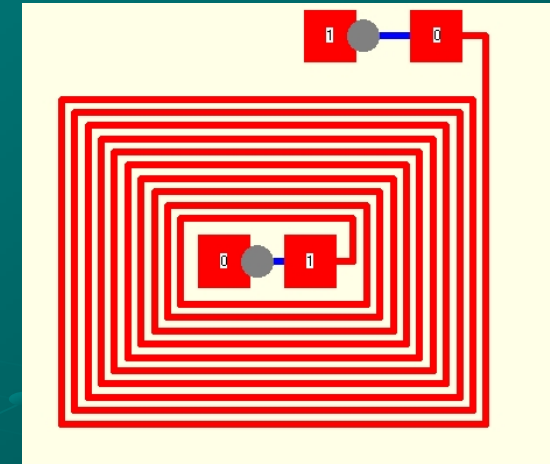
$$\nabla^2 \mathbf{A}_b - \gamma^2 \mathbf{A}_b = 0 \quad \text{in region } R_b$$

$$\gamma = j\omega\mu\sigma$$



# The model

Coil Impedance:  $Z = Z_0 + \Delta Z$



$$\Delta Z_{Coil\ 1,2} =$$

$$\frac{j8\omega\mu_0}{\pi^2(z_2 - z_1)^2 c^2} \int_0^{+\infty} \int_0^{-\infty} \frac{\left[ \sum_{i=1}^n \Gamma(x_{c,i}, y_{c,i}) \right]^2}{(\alpha\beta)^2} \frac{\left[ e^{-kz_{1,u}} - e^{-kz_{2,u}} + e^{-kz_{1,d}} - e^{-kz_{2,d}} \right]^2}{k} d\alpha d\beta$$

2 layer flat rectangular coil



$$g = 1 - \mu_r k / \lambda$$

$$k^2 = \alpha^2 + \beta^2$$

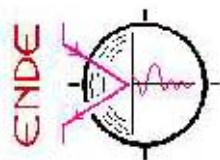
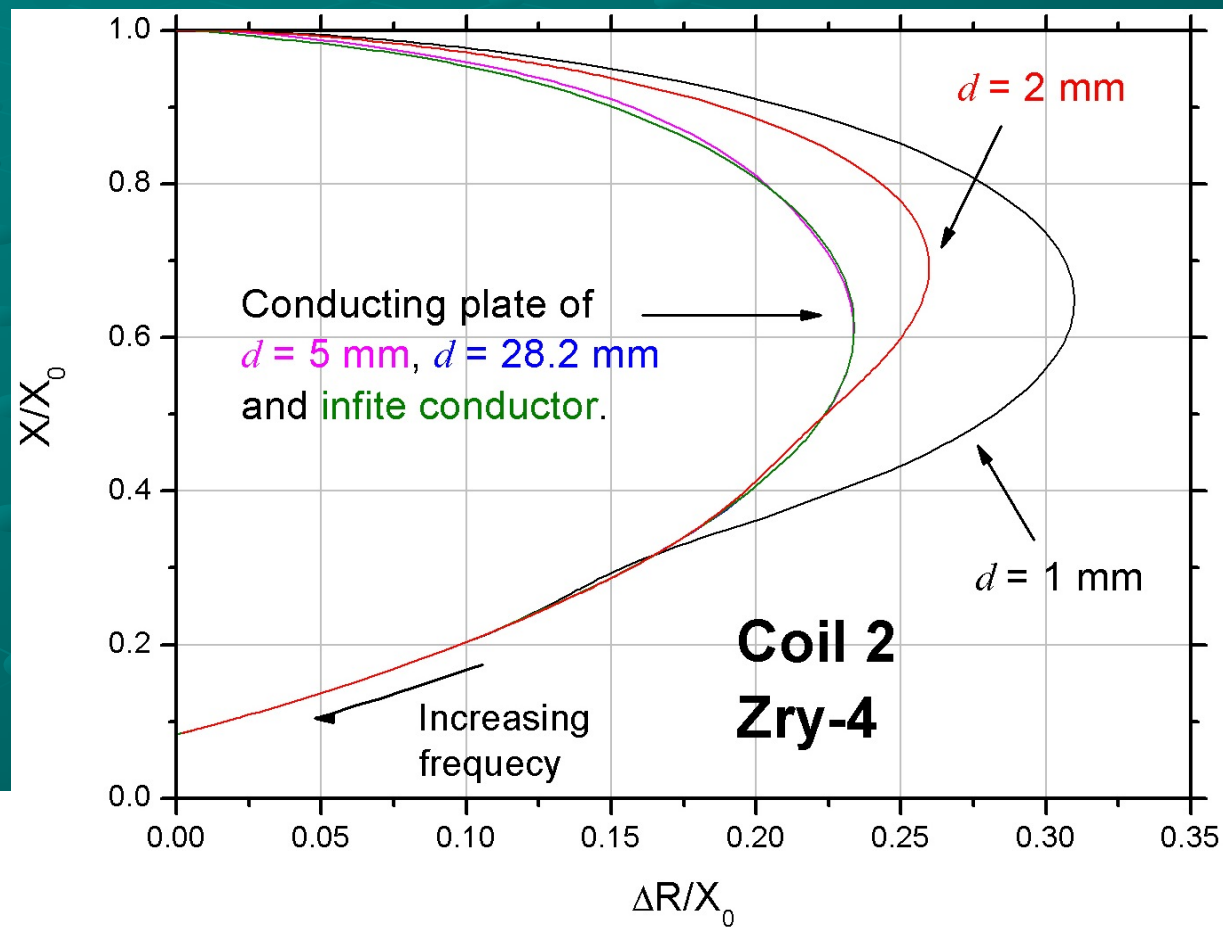
$$h = 1 + \mu_r k / \lambda$$

$$\lambda^2 = k^2 + \gamma^2$$



# Z-diagram of a finite thickness conducting plate

(comparison with a semi infinite conducting block)

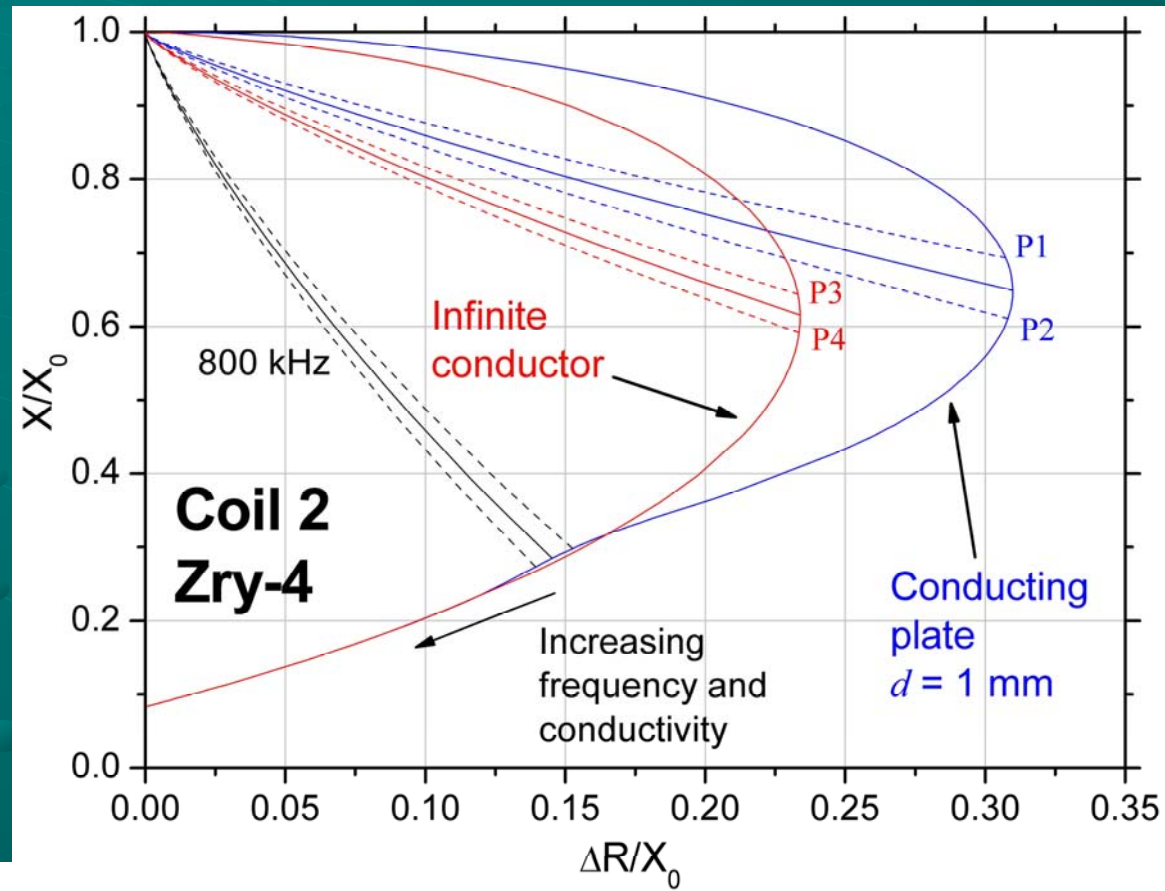


ENSAYOS NO DESTRUCTIVOS y ESTRUCTURALES

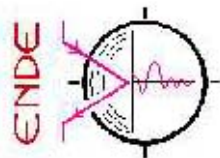
$F_{\max} = 10 \text{ MHz}$



# Calculated Z- diagram: Study of effect of $\sigma$ and thickness



$F_1 = 75$  kHz  
 $F_2 = 800$  kHz



ENSAYOS NO DESTRUCTIVOS y ESTRUCTURALES

$F_{\max} = 10$  MHz



# Summing up

- An analytical solution to the problem of calculating the EM fields produced by a flat rectangular eddy current coil above a conducting plate was presented.
- At the limit for thick specimens the new calculations coincide with those for the infinite block.
- From the calculations, it can be defined the minimum thickness a particular conducting material should have in order to be considered infinitely thick for an EC test, i.e. at a given test frequency.
- For these coils, a 5 mm thick material “is” infinitely thick in all the frequency range for EC, independent of its conductivity.
- The coils have a better coupling to a thin plate than to a thick one.



Introduction

Material characterization

Basic work:

Corrosion of Zr-base alloys

Steels

Eddy currents testing: probe design

Modelling

Evaluation of damage

Review of literature on Zr hydrides

International projects:

IAEA – CRP

NIRDTP

IZFP

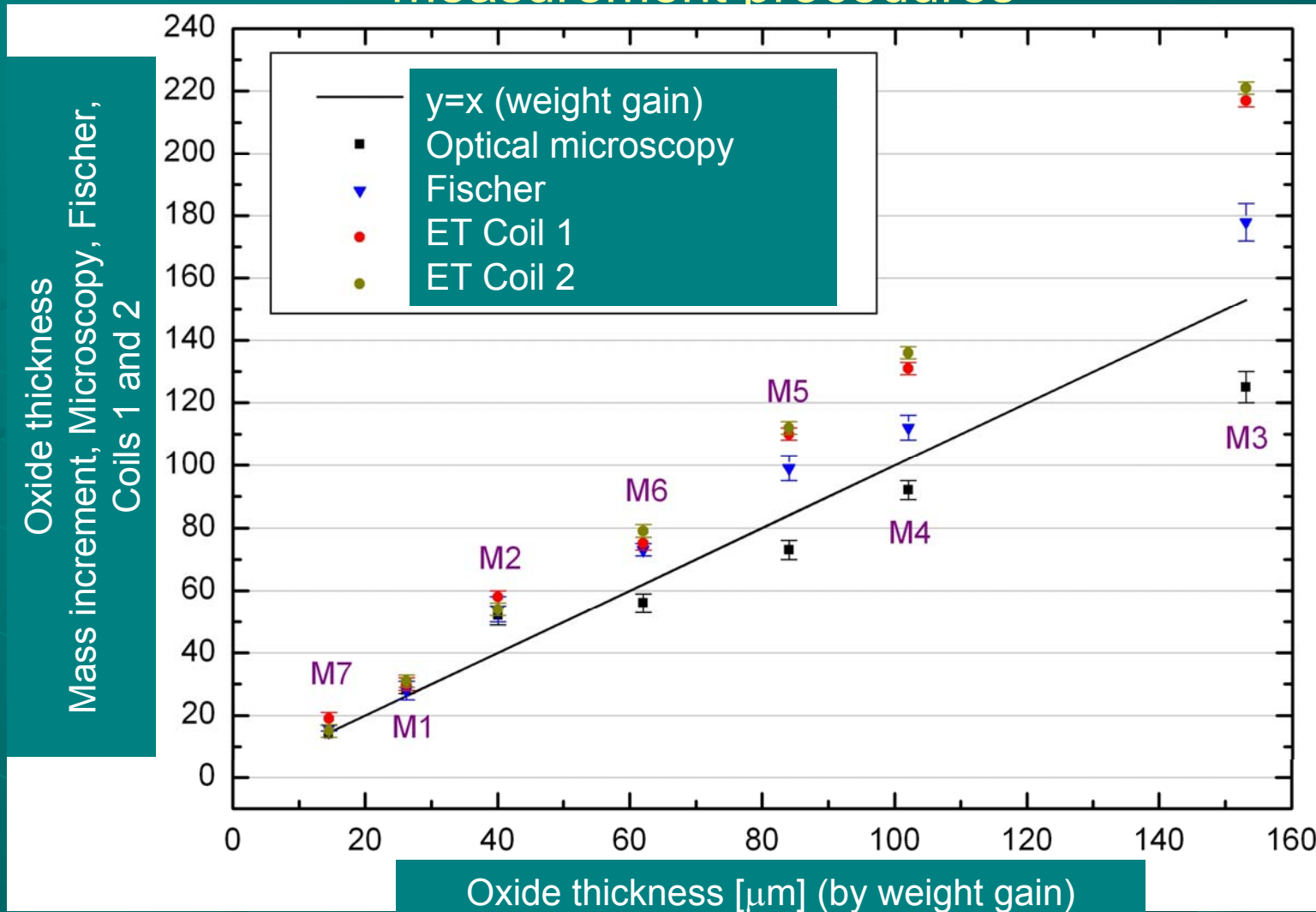
# Evaluation of autoclave treated Zry-4

- Thickness of oxide layer: weight gain; Fischer thickness gauge; optical microscopy
- Hydrogen content: eddy-currents: Z-plane with ect and calibration standards; model and Solartron 1260 Z-analyzer; Fischer Conductivity gauge. X-ray diffraction; direct extraction with LECO.
- By eddy currents, the thick specimens could be classified in three groups according to their H content

# Autoclave treatment of Zircaloy-4 in 1M LiOH at 340°C and equilibrium pressure 13.6 MPa

	M7	M1	M2	M6	M5	M4	M3
Specific weight gain [mg/dm <sup>2</sup> ]	233	416	683	1018	1392	1658	2496
Oxide thickness [μm]	17	30	53	75	103	106	172
Hydrogen [wt ppm]	142	231	687	835	1204	1296	2019

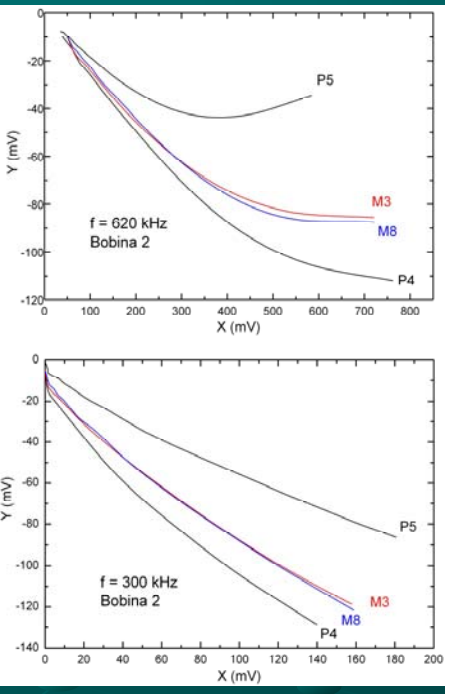
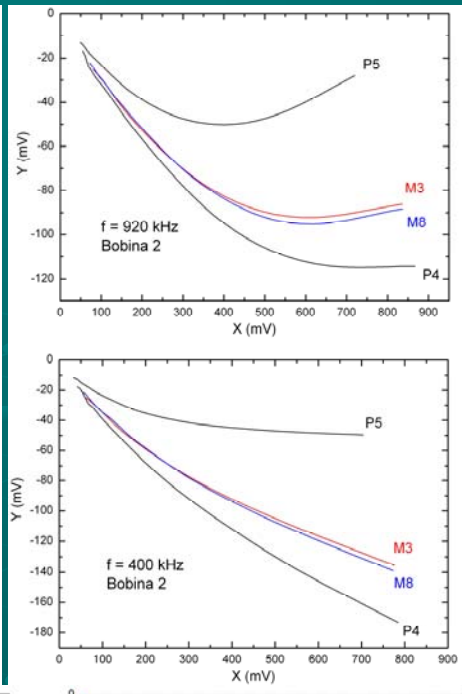
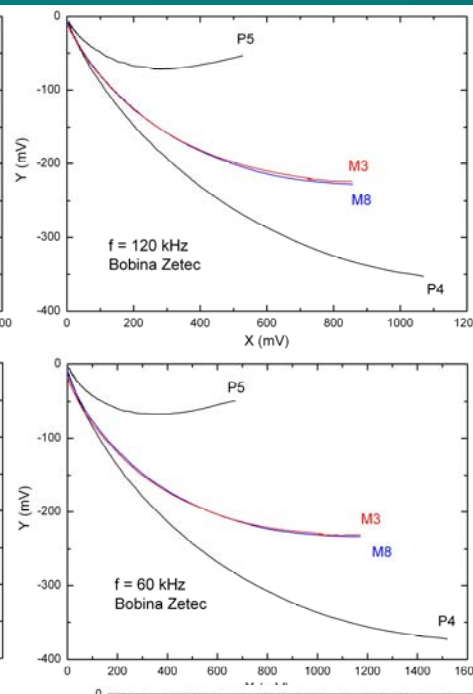
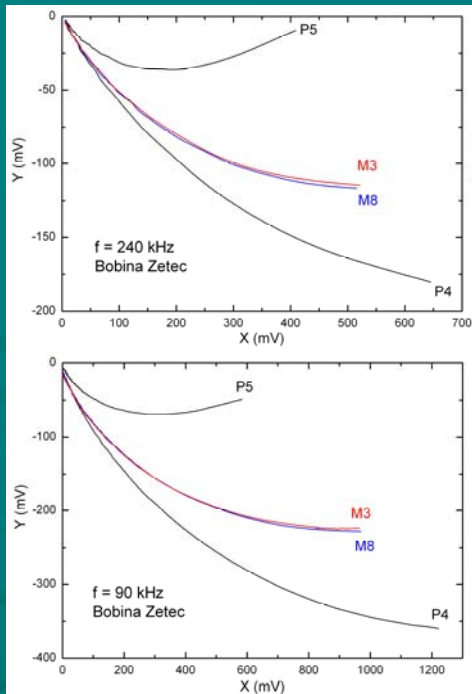
# Oxide thickness [ $\mu\text{m}$ ]: comparison of different measurement procedures



Weight gain indicates average oxide thickness.

Fischer Dualscope MP40 measures oxide thickness at particular points.

ET coils + model indicate maximum oxide thickness in each specimen.

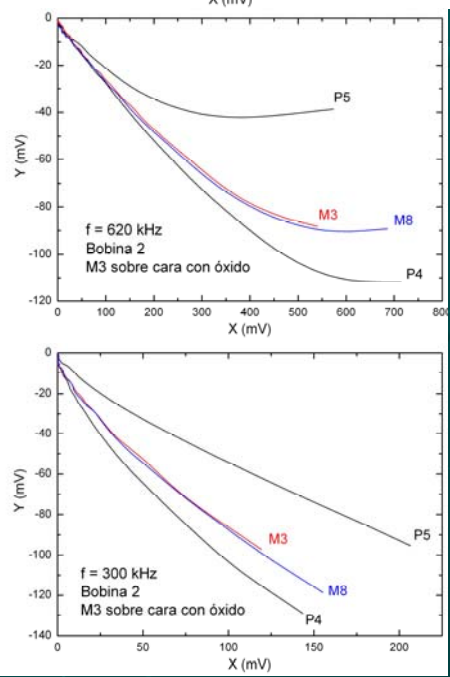
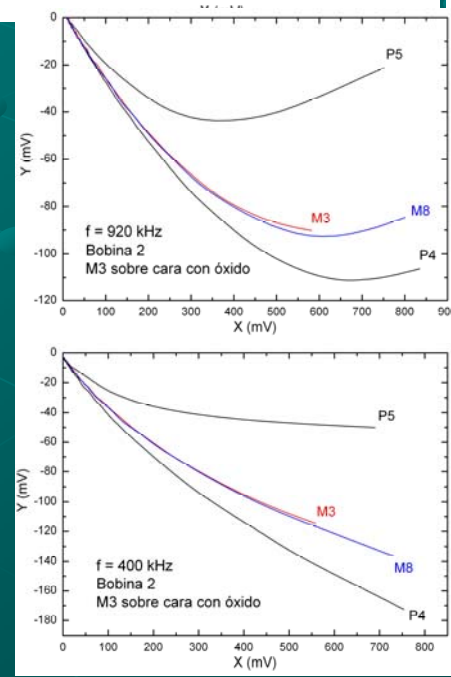


Pancake coil Zetec  
(above left)

ET, MAD 8D from  
ECT

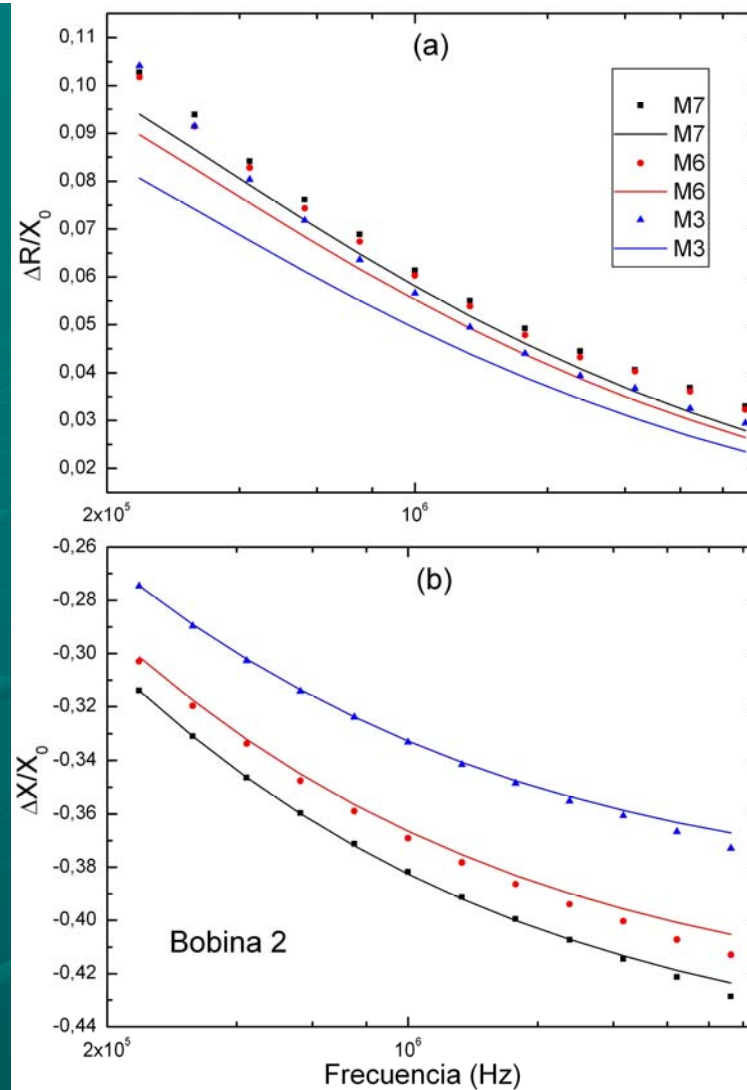
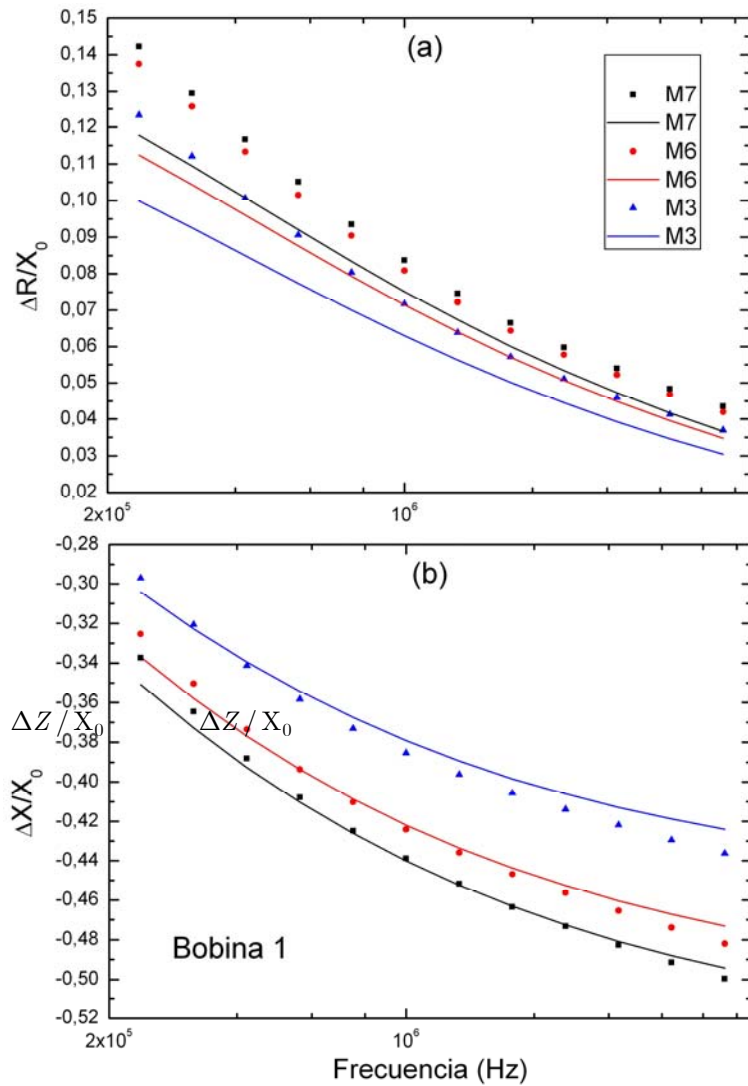
Z-plane indications  
from autoclave  
corroded thick  
specimens.

Effect of H content



Planar coil  
Oxide free face  
(above right)

Oxide face  
(left)



Normalized impedance  $\Delta Z(f)$  - planar coils.  
 Dots: corrected experimental data;  
 Full lines: Calculated values.  
 Thick specimens could be classified in three groups,  
 according to conductivity and hydrogen content

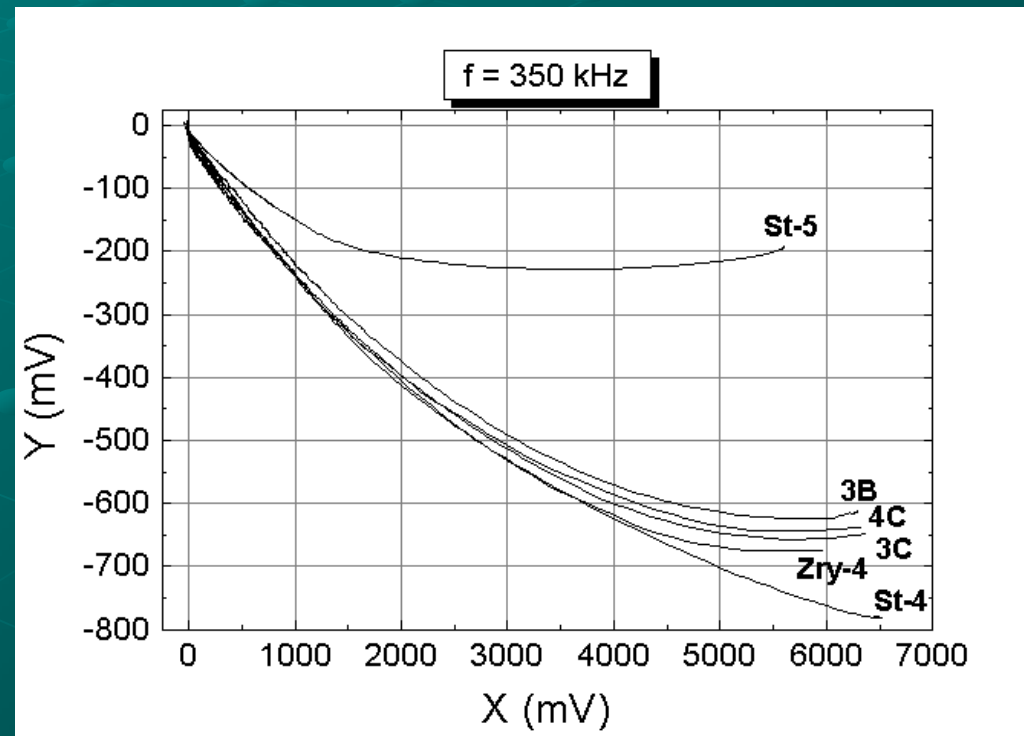
Modelling: SOVP  
 second order vector  
 potential method

# H content in Zircaloy-4 - eddy currents

Thin specimens (1 mm thick)

Impedance plane curves

Sample	[H] (wt-ppm)	Resistivity ( $\mu\Omega\text{cm}$ )
3C	$565 \pm 65$	$71 \pm 1$
4C	$870 \pm 90$	$75 \pm 1$
3B	$1520 \pm 150$	$76 \pm 1$



# Hydrogen assessment: Conductivity measurements Conclusions

- The 5 mm thick specimens could be classified in three groups in terms of hydrogen content.
- Better sensitivity was obtained with 1 mm thick specimens.
- Effect of hydride distribution in specimen thickness to be studied.
- Combined influence of conductivity and thickness.

Introduction

Material characterization

Basic work:

Corrosion of Zr-base alloys

Steels

Eddy currents testing: probe design

Modelling

Evaluation of damage

Review of literature on Zr hydrides

International projects:

IAEA – CRP

NIRDTP

IZFP

# Characterization of Cold Rolling-Induced Martensite in Austenitic Stainless Steels

Marta Clelia RUCH <sup>1</sup>, Javier FAVA <sup>1</sup>, Cristina SPINOSA <sup>1</sup>, Monica LANDAU <sup>1</sup>,  
Guillermo COSARINSKY <sup>1</sup>, Adriana SAVIN <sup>2</sup>, Frantisek NOVY <sup>3</sup>,  
Vitalja TURCHENKO <sup>4</sup>, Mihail Liviu CRAUS <sup>4</sup>

<sup>1</sup> Comision Nacional de Energia Atomica, San Martin - Buenos Aires, Argentina

<sup>2</sup> National Institute of R&D for Technical Physics, Iasi, Romania

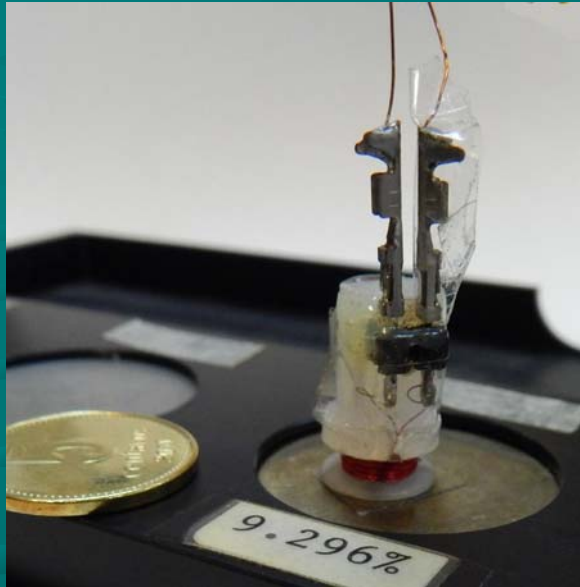
<sup>3</sup> University of Žilina, Žilina, Slovakia

<sup>4</sup> Joint Institute for Nuclear Research, Dubna, Russia

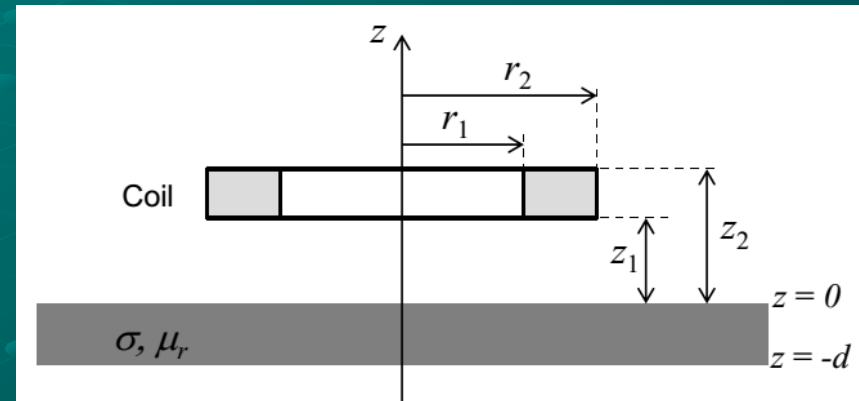
Contact e-mail: [ruch@cnea.gov.ar](mailto:ruch@cnea.gov.ar)



# Eddy currents – assessment of $\mu$



With a Solartron 1260 impedance analyzer, the impedance of a coil with an alternate current of frequency  $f$  is measured in air and coupled to a conducting specimen, thus obtaining the experimental impedance difference  $\Delta Z^E$  as a function of  $f$ .



The theoretical impedance difference  $\Delta Z^T$  of the coil in air and on the specimen is calculated with the model.

Procedure for conductivity calculation

Coupling  
 $z_1 = \text{lift-off}$

Coil  
 $\{N, r_1, r_2, (z_2 - z_1)\}$

Specimen  
 $\{\sigma, \mu, d\}$

Theoretical model

Impedance analyzer

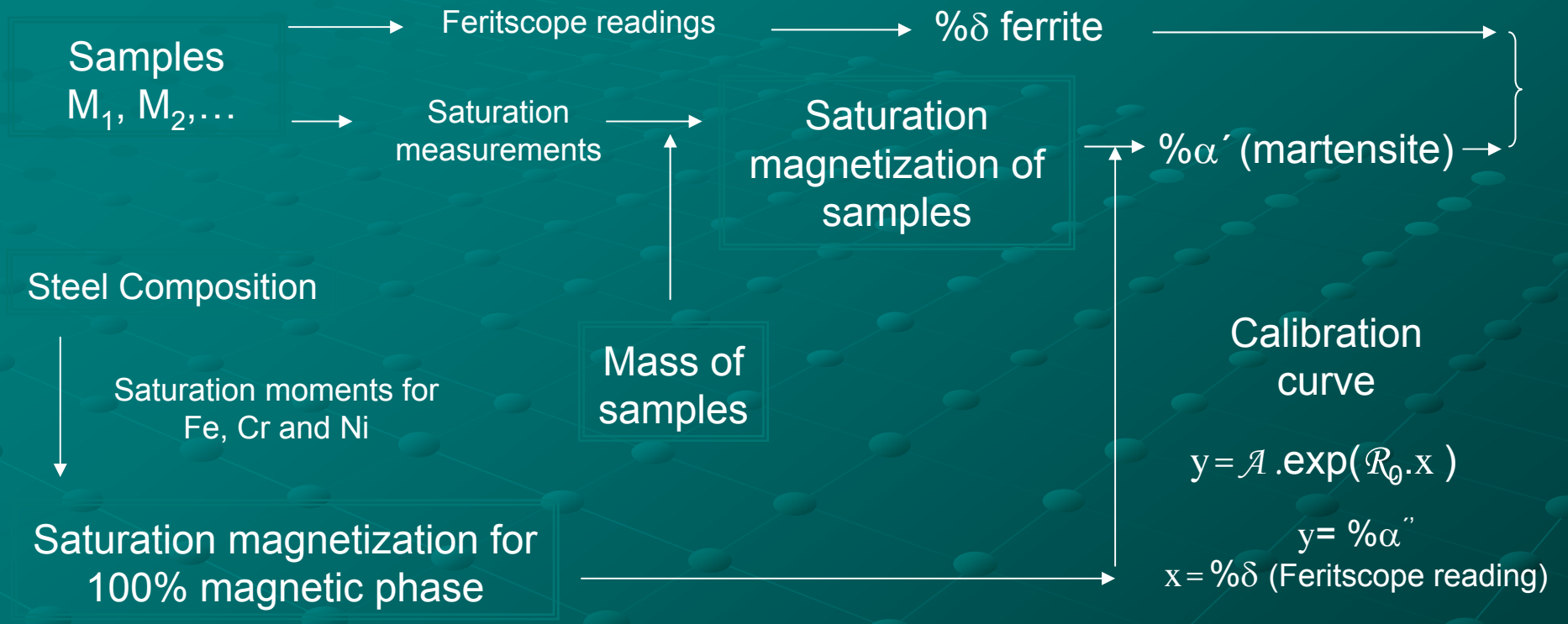
$$\Delta Z^T = Z^T - Z_0^T = F(N, r_1, r_2, z_1, z_2, f, \sigma, \mu, d)$$

$$\Delta Z^E = Z_{\text{Corr}}^U - Z_0$$

Least square fitting

Assessment of  $\{\sigma, \mu, (z_2 - z_1)\}$

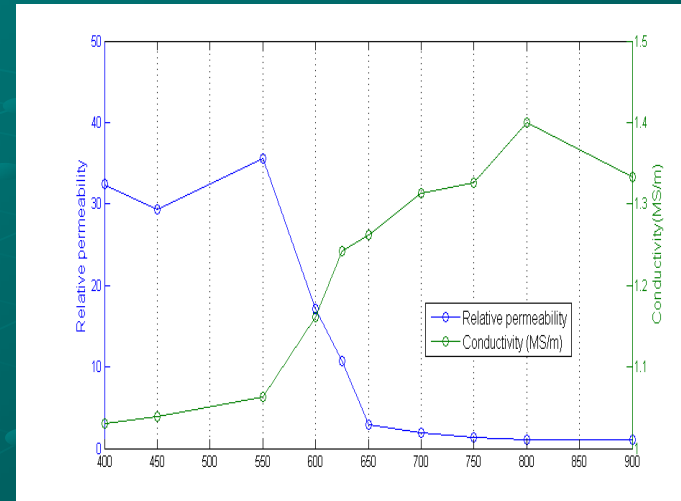
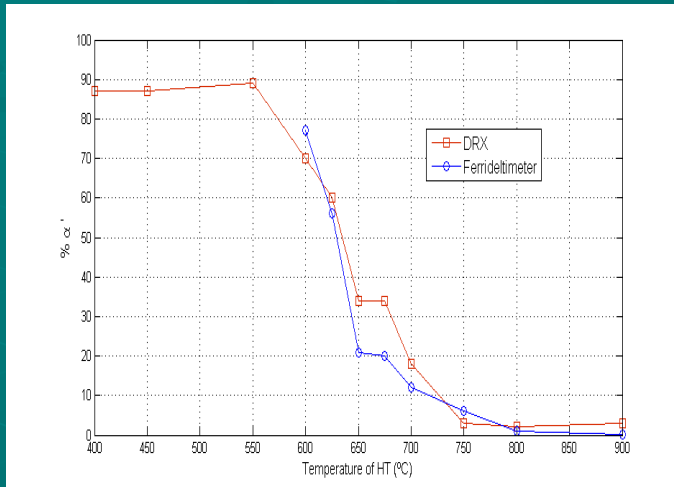
# Procedure for magnetic measurements



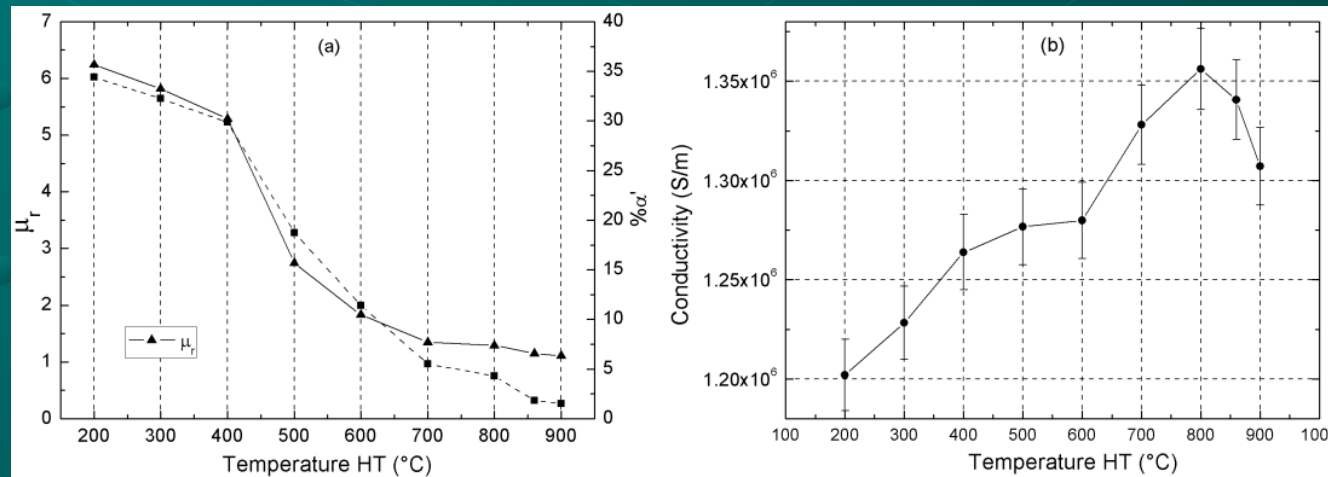
# Phase content, DRX- Ferrideltimeter

## Relative permeability and electrical conductivity of HT specimens, measured at RT

304



316



# Conclusions

- Techniques recently available in the lab were used to improve previous results on specimens of metastable 304 and 316 austenitic SS. Traditional techniques were also used.
- Reversion of martensite was studied with XRD, Feritscope, metallography, eddy-currents plus a model (magnetic permeability), electrical conductivity (van der Pauw) and Vickers microhardness.
- The phase transformation process could be studied at RT using specimens which had been submitted to reversion HT using all of the above mentioned methods.
- The conductivity curve showed a two-stage reversion process.
- Diffusion reversion could start at 550°C and shear reversion at 650°C
- The metallographic studies showed the deformed faulty structure of the fcc' phase.
- Full reversion to austenite was not achieved with the 1 hour HT at any temperature reported here.
- Recrystallization was active at 800°C
- 316 proved to be less sensitive to DIM than 304

Introduction

Material characterization

Basic work:

Corrosion of Zr-base alloys

Eddy currents testing: probe design

Modelling

Steels

Evaluation of damage

Review of literature on Zr hydrides

International projects:

IAEA – CRP

NIRDTP

IZFP

Comments on the stability of zirconium hydride phases in Zircaloy  
L. Lanzani, M. Ruch  
Journal of Nuclear Materials 324 (2004) 165–176

Autoclave treated Zircaloy-4 specimens were submitted to different XRD experiments for a period of about 3 years, in order to study the stability of the hydride phases.

A thorough review of the literature about hydride phases in pure Zirconium and Zirconium-base alloys was made.

In our Zircaloy-4 specimens, only delta-hydride was observed.

Conditions for the formation of gamma-hydride in high purity Zr and alloys with beta stabilizers is discussed in the paper. Here only the conclusions are presented,

## Comments on the stability of zirconium hydride phases in Zircaloy

L. Lanzani, M. Ruch

Journal of Nuclear Materials 324 (2004) 165–176

- Only delta-hydride is detected by XRD after autoclave hydriding Zircaloy-4 at 340°C in LiOH for  $C_H > 100$  wt ppm. Chemical etching was avoided throughout.
- Within the detection limit of XRD, none of the characteristic diffraction peaks of the gamma-hydride were observed either after autoclaving or after aging at 148°C and RT.
- The literature shows experimental evidence that gamma-hydride is an equilibrium phase in high purity zirconium, while in less pure zirconium and alpha-zirconium alloys, gamma-hydride is a metastable phase.
- The presence of alpha-stabilizers favors the growth of delta-hydride (hardening effects).
- Nuclear grade Zircaloy-4 should contain principally delta-hydride as a stable phase.
- The anomalies in the dynamic studies in Zr–2.5%Nb might be related to similar effects reported in high purity zirconium.
- A study of the ternary system Zr–Nb–H might help in the analysis of the stability of hydride phases in zirconium–niobium alloys.

Introduction

**Material characterization**

Basic work:

Corrosion of Zr-base alloys

Eddy currents testing: probe design

Modelling

Steels

Evaluation of damage

Review of literature on Zr hydrides

**International projects:**

**IAEA – CRP**

NIRDTP

IZFP



IV Conferencia Panamericana de END  
Buenos Aires – Octubre 2007

# Pressure Tubes Blister Detection by NDT

G. Domizzi, A. García, M. Ruch, C.  
Desimone, J. Fava, C. Belinco

Comisión Nacional de Energía Atómica  
Argentina



# **IAEA Co-ordinated Research Project**

**Argentina - Canada - India- - Korea - Romania**

## **OBJECTIVE:**

**to assess the capability of different destructive and non destructive techniques to measure (H&D) concentration and to characterize hydride blisters in pressure tube material**



## Specimens and Techniques for evaluation of Hydrogen content

150 specimens with H content ranging from 20 to 100 wt-ppm were prepared for the 5 partner countries and the different assessment techniques:

Inert Gas Fusion (IGF),

Hot Vacuum Extraction Mass Spectrometry (HVEMS),

Ultrasound (UT)

Eddy Currents (ET)

Differential Scanning Calorimetry (DSC)

Differential Thermal Analysis (DTA)

Resistivity



## Zr-2.5 Nb was hydrided by cathodic charge

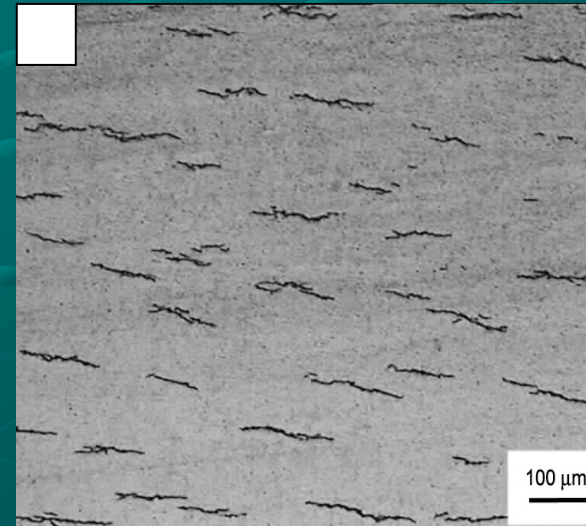
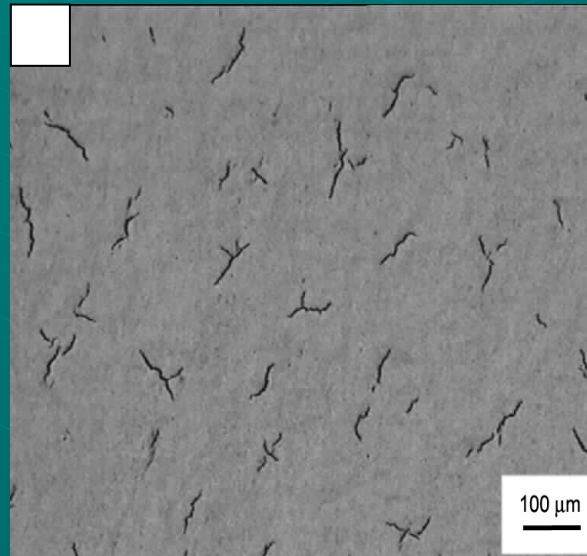
- Clean fast method.
- Conditions are different from in pile corrosion.
- No oxide is formed in the process.
- A hydride layer is formed: diffusion HT are necessary.
- Kinetics of hydriding determined by temperature of the process.
- Hydrides in specimens for NDT and the construction of calorimetric curve of terminal solid solution (TSS) must have the same distribution as those formed during in-pile corrosion at 340°C
- Hydrides in specimens for extraction techniques may have any distribution. (Higher temperatures allowed)

# Zirconium hydrides in Zr-2.5Nb

## Hydride distribution

Charging in alpha+beta

Charging in alpha



radial  
↑  
transversal  
→

↓  
Suitable for NDT and TSS  
(terminal solid solubility)  
curve determination

IV PANNDT - Pressure Tubes  
Blister Detection by NDT



# Hydride blisters in Zr-2.5Nb

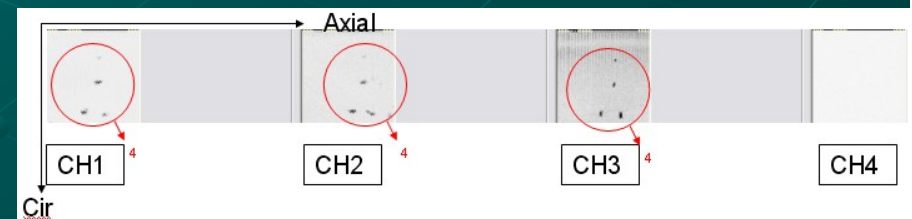
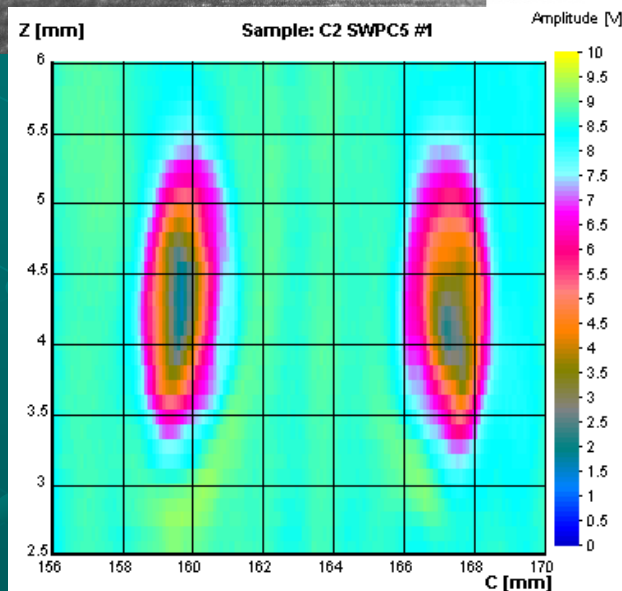
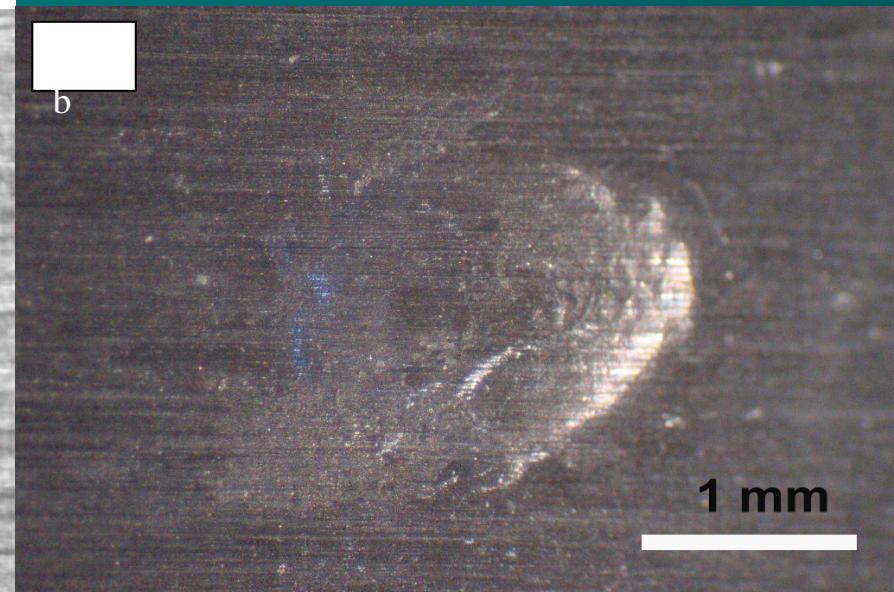
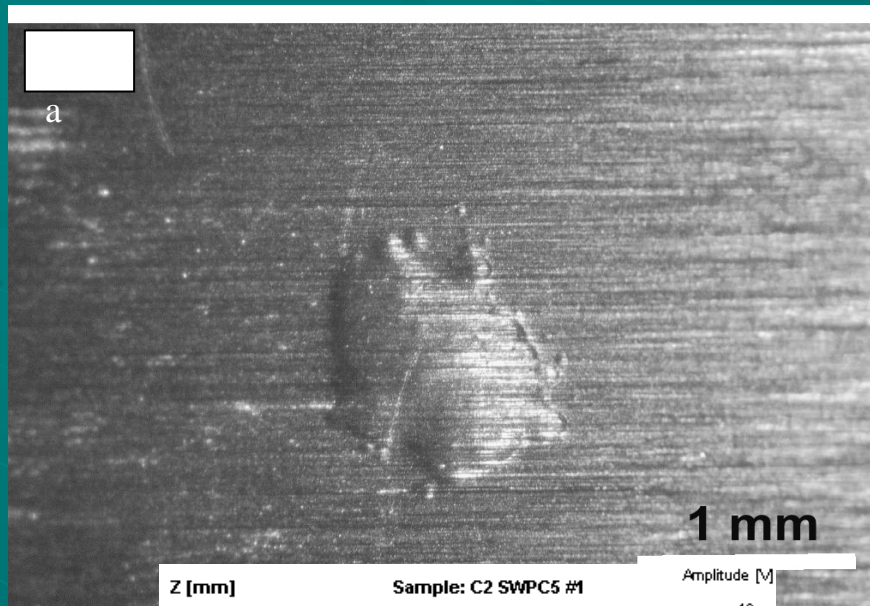
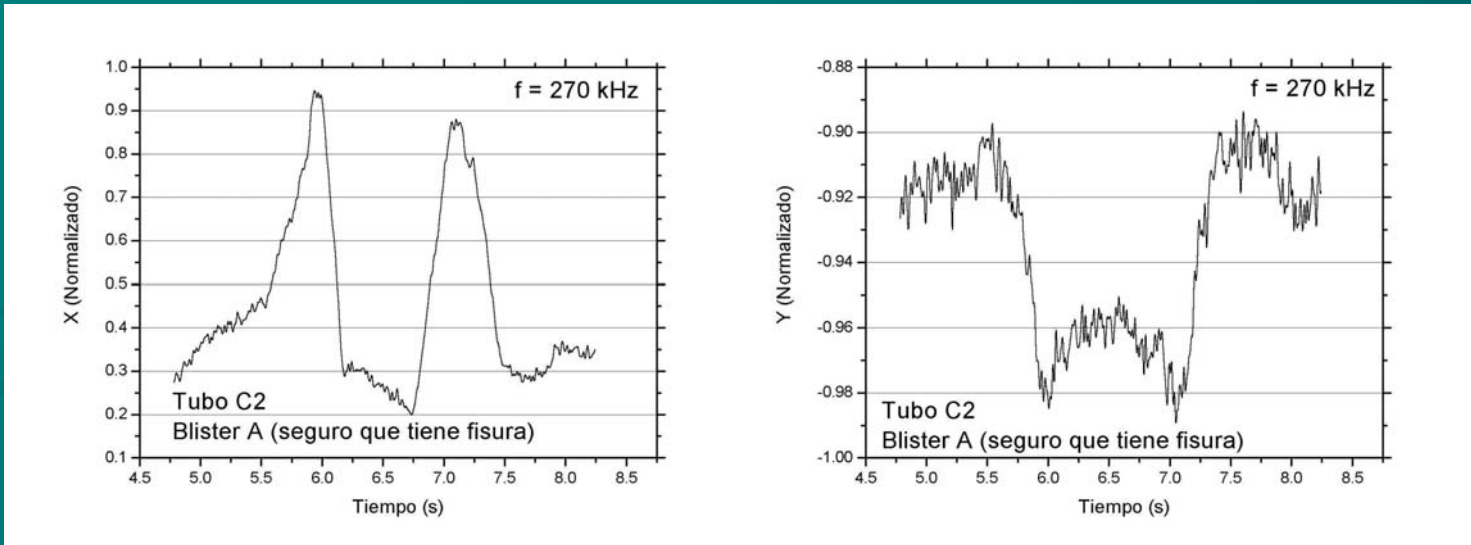
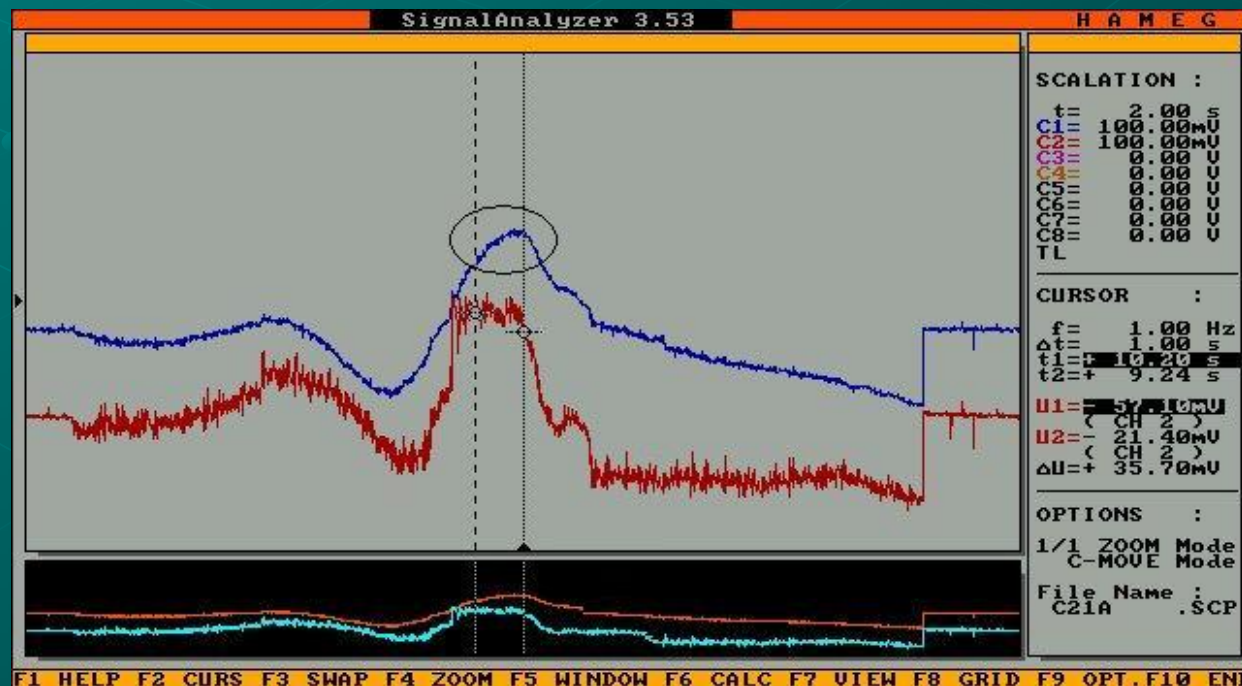


Fig. 3.3.10.4. PC amplitude image of the blister C2-b



## Eddy currents X(T) Y(t) signals for blister *a* in C2.



# CONCLUSIONS

- In the framework of an IAEA co-ordinated research Program an important effort was made to produce standards for hydrogen concentration measurement and to inter-compare different techniques usually applied to construct terminal solid solubility curves
- The hydride dissolution temperatures measured agree better with the  $T_d$  calculated from the SST curves reported by Pan et al, McMinn, Slattery and Jovanovic than with that from Kearns.
- Blisters were formed on PT sections in order to assess the detection sensitivity of different ND techniques.
- Blister detection was accomplished with UT from the inside of PT and with Eddy Current from the outside of PT. Further work with EC is necessary for detection from the inside



Introduction

## Material characterization

Basic work:

Corrosion of Zr-base alloys

Eddy currents testing: probe design

Modelling

Steels

Evaluation of damage

Review of literature on Zr hydrides

## International projects:

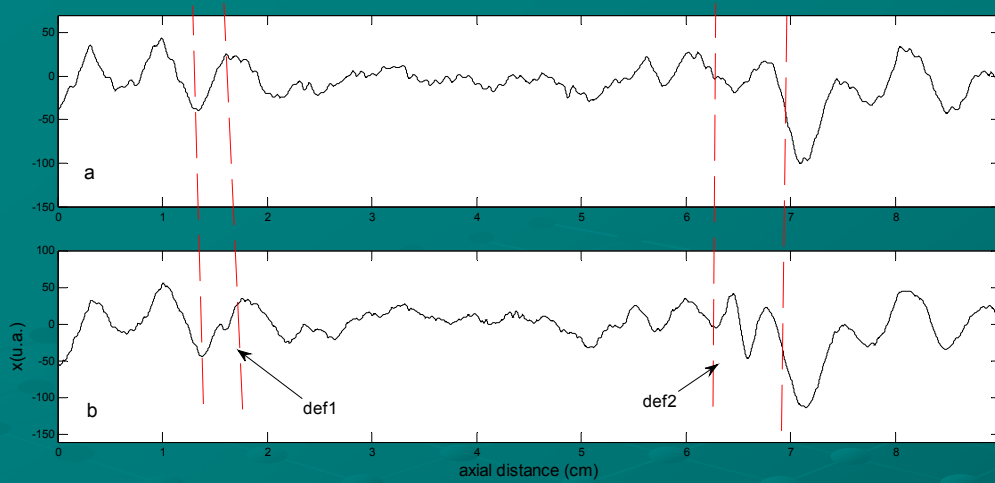
IAEA – CRP

NIRDTP

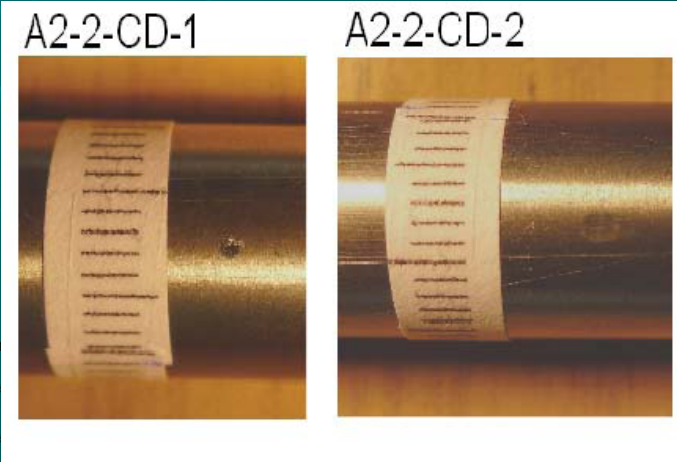
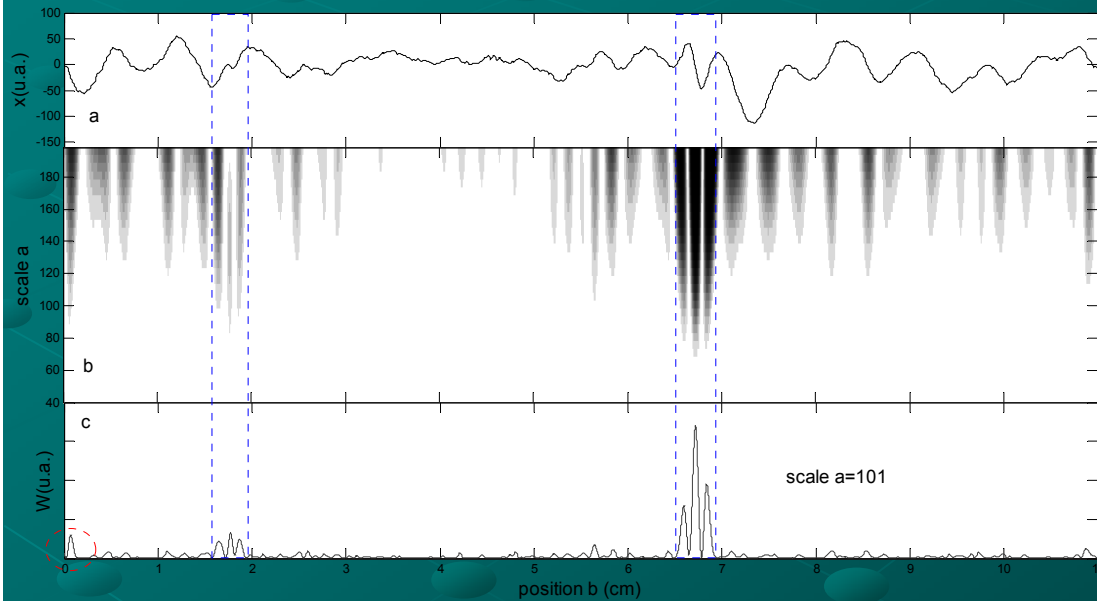
IZFP

**Eddy current testing reliability improvement;  
application to nuclear fuel cladding tubes**

G.Cosarinsky, M.Ruch, G.Rugirello, G.Domizzi,  
A.Savin, R.Steigmann, R.Grimberg  
Comisión Nacional de Energía Atómica,  
Centro Atómico Constituyentes, Buenos Aires, Argentina  
National Institute of R&D for Technical Physics,  
Nondestructive Testing Department, Iasi, Romania



Two ET inspections of a cladding, before (a) and after (b) generating two artificial defects on its external wall.



Continuous Wavelet Transform (CWT) of the above signal. Defect indications can be clearly seen,

Introduction

**Material characterization**

Basic work:

Corrosion of Zr-base alloys

Eddy currents testing: probe design

Modelling

Steels

Evaluation of damage

Review of literature on Zr hydrides

**International projects:**

IAEA – CRP

NIRDTP

**IZFP**



# Non destructive characterization of laser hardened steels

**Bilateral cooperation project: MINCYT-BMBF AL-1109**

Argentina-MINCYT (Ministerio de Ciencia, Tecnología e Innovación Productiva)  
Science, Technology and Innovation

Deutschland-BMBF (Bundesministerium für Bildung und Forschung)

G. Cosarinsky<sup>(1)</sup>, M. Kopp<sup>(2)</sup>, M. Rabung<sup>(2)</sup>, G. Seiler<sup>(3)</sup>, A. Petragalli<sup>(1)</sup>, D. Vega<sup>(1)</sup>, M. Sheikh-Amiri<sup>(3)</sup>, M. Ruch<sup>(1)</sup>, C. Boller<sup>(3)</sup>

<sup>(1)</sup> CNEA – Buenos Aires, Argentina

<sup>(2)</sup> IZFP, Saarbrücken, Germany

<sup>(3)</sup> Universität Saarland, Saarbrücken, Germany

cosarinsky@cnea.gov.ar

# Objetives

- To characterize laser hardened steel specimens using different techniques
- To study the performance of 3MA in the assessment of residual stresses
- Materials: Structural steels C45 (1045); 50CrMo4 (AISI 4150); 42CrMo4 (AISI 4140 or 4142)

Characterization tests performed at CNEA (G. Cosarinsky, A. Petragalli, D. Vega, G. Seiler, M. Sheikh-Amiri, M. Ruch)

1. X-Ray diffraction: crystal structure, phases present, residual stresses
2. Metallography
3. Optical and scanning electron microscopy

Characterization tests performed at IZFP (G. Cosarinsky, M. Kopp, M. Rabung, G. Seiler, M. Sheikh-Amiri, C. Boller)

1. 3MA KK6 Micromagnetic Multiparametric Analysis of Microstructure and Stresses, with VGB probe, at a magnetization frequency of 150 Hz;
  - 1.1. MagAmp scans to find optimal test conditions.
  - 1.2. Scans on the samples. Automatic positioning. MagAmp 30 and 80 Amp/cm; magnetization frequency = 150 Hz
2. Hardness measurements with Krautkrämer TIV (Through Indenter Viewing)
3. Point probe measurements

# Laser hardening

- A surface engineering technique, which uses a focused energy beam to produce a controlled localized heating followed by self-quenching.
- Surface hardening is achieved through a martensitic transformation down to a limited depth, without affecting all the thickness of the piece.
- Laser hardening improves wear resistance
- Very short thermal cycle: resulting microstructures in the laser treated zone can differ considerably from those obtained by traditional heat treatments.

# Laser hardened samples

Materials: C45, 50CrMo4, 42CrMo4, 34CrMo4, 25CrMo4

Each sample has a hardened strip, with different values of laser temperature and laser speed

50CrMo4	temp				
speed		0.2	0.3	0.5	0.7
	1000	17			
	1100	1	2	3	4
	1200	5	6	7	
	1300	9			
	1400	13			
	1420	15			

42CrMo4	temp				
speed		0.3	0.7	1	2
	1000	1003	1007	11	
	1100	no number	1107-22	1110-22	1120
	1200		61	1210	
	1300	1303	1307		

— x ray sample, not scanned  
temp (°C)  
speed (m/min)

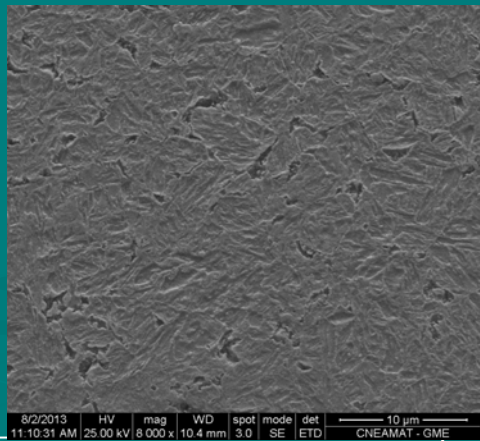
LI = lowest intensity  
HI = highest intensity

C45	temp		
speed		0.3	0.5
	1000	8,3	8,4
	1050	7,3	7,4
	1100	6,3	6,4
	1150	5,3	5,4
	1200	4,3	4,4

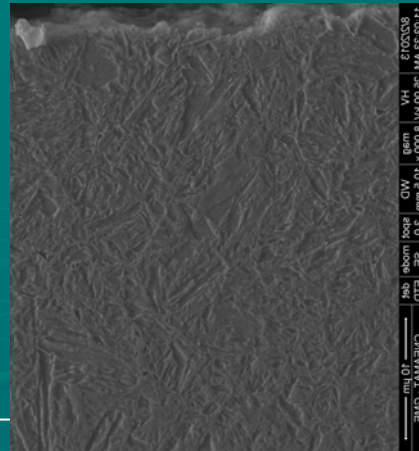
Numbers in the cells are  
sample names



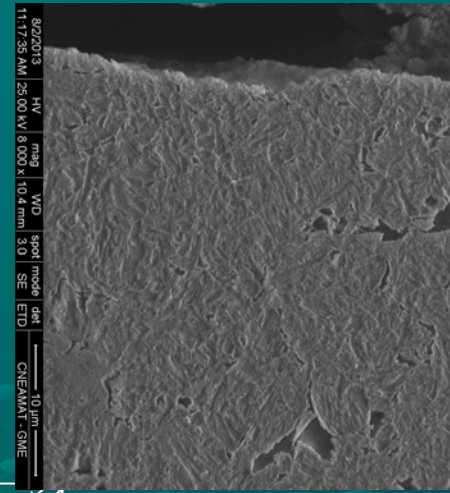
# Martensite needles



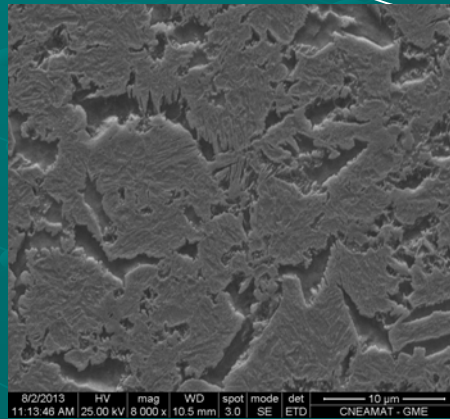
LHZ



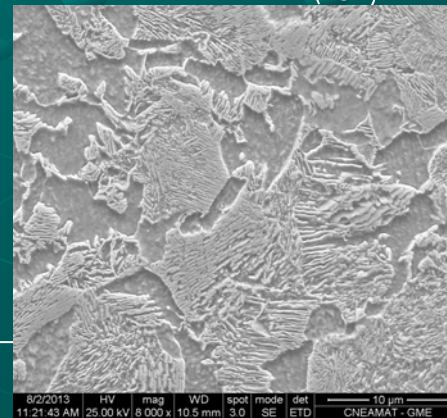
HAZ. Fine martensite. Ferrite



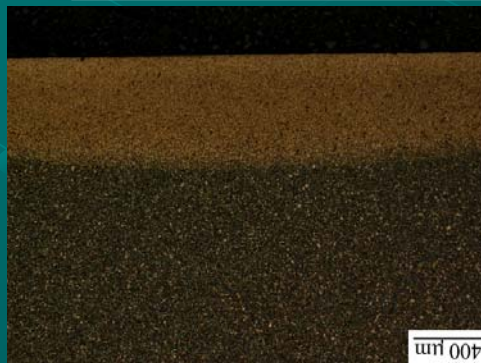
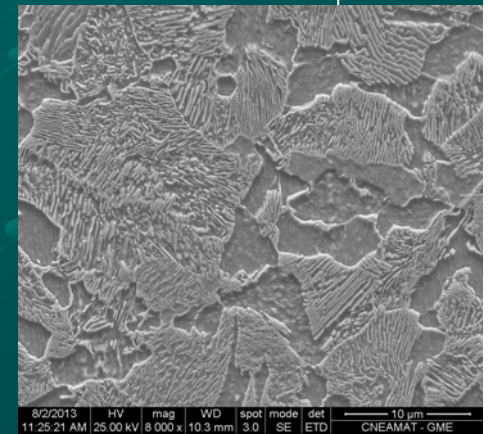
Martensite.  
Retained austenite



HAZ-Ferrite.  
Martensite

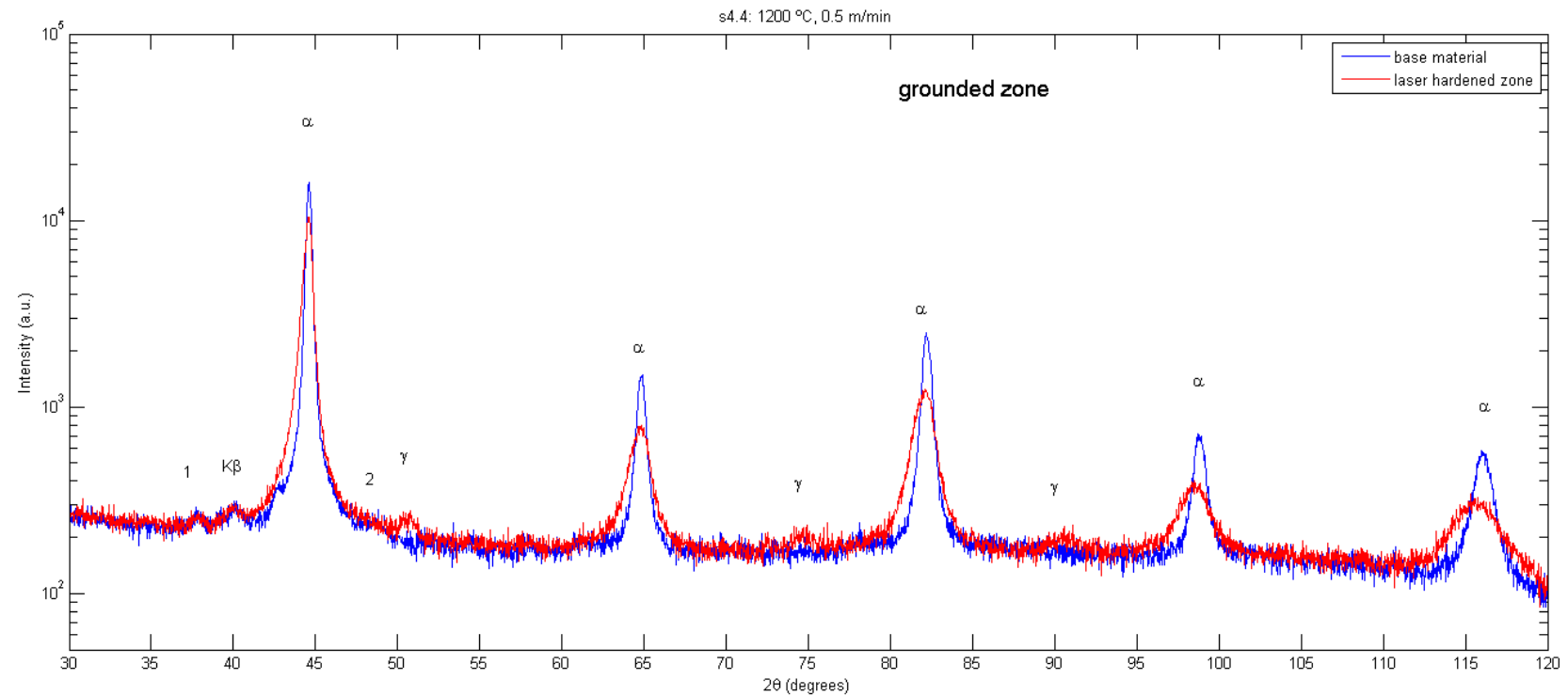


Base material.  
Pearlite. Ferrite.



SEM - C45 – sample 44 – 1200 °C – 5 dm/min

# X-ray diffraction of Sample 44 – 1200°C – 5 dm/min polished. Comparison of base metal and laser hardened zone

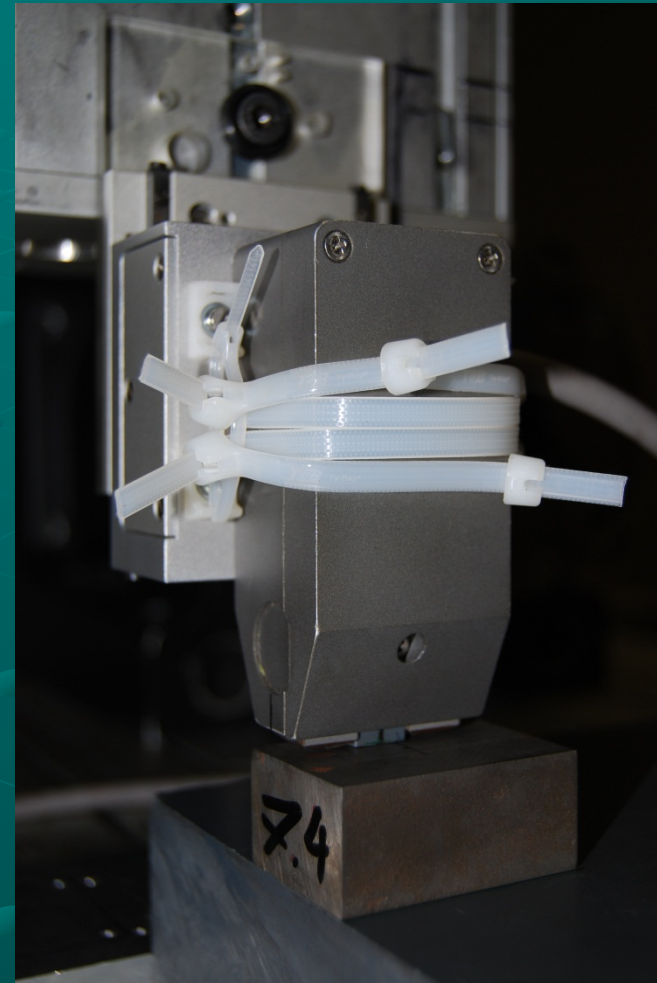
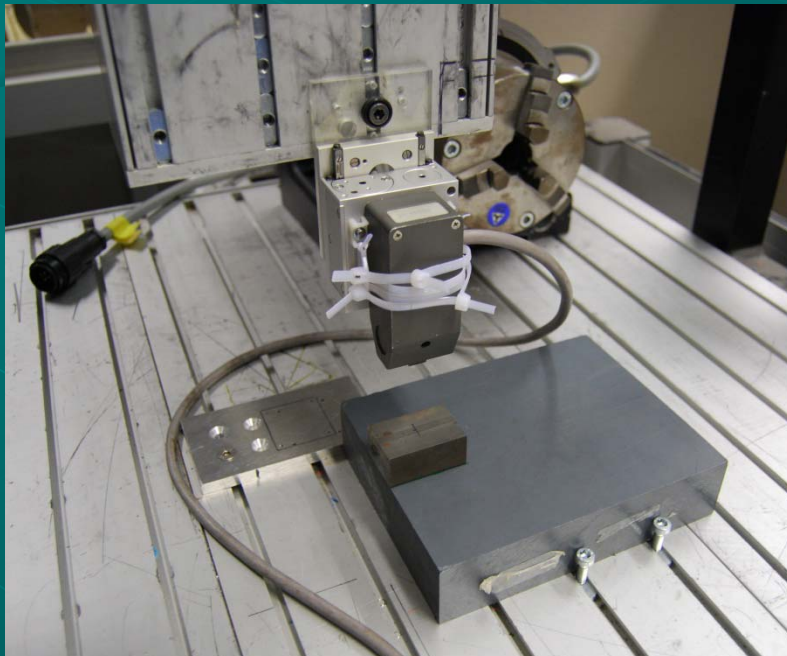


## SCANS with 3MA

The scans were made with two  
MagAmp values: 30 A/cm and 80 A/cm

The scan direction is perpendicular to  
the hardened strip

Resolution: 4 pixels/mm

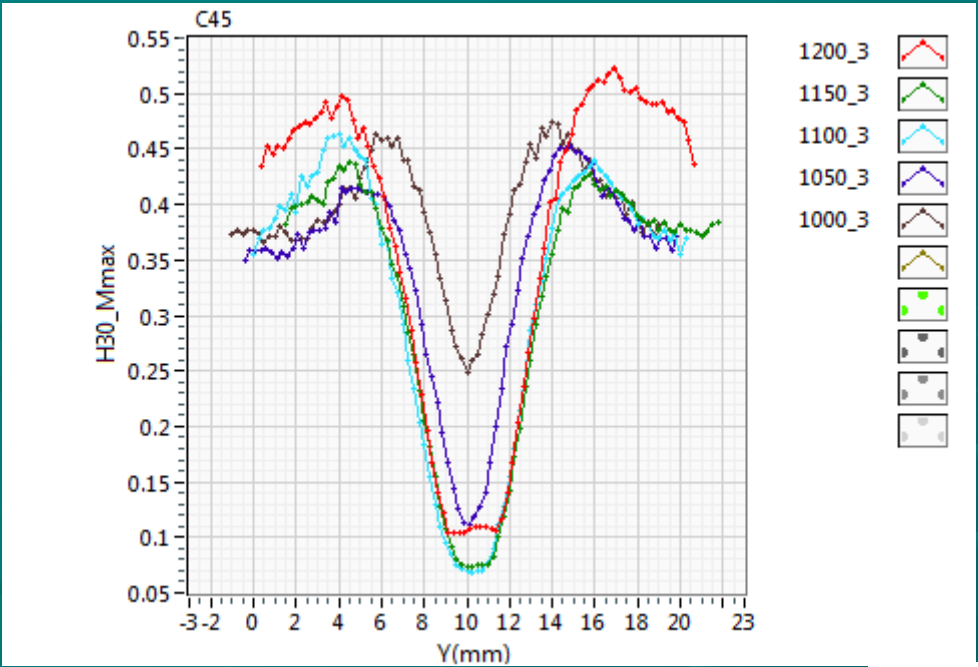


# Barkhausen noise experiments

- Although many parameters of the magnetic behaviour of the samples were recorded in the experiments, we are presenting only two characteristic parameters of Barkhausen noise signals:  $M_{\max}$  and  $H_{\text{cm}}$ ,
  - $M_{\max}$  the maximum amplitude of the Barkhausen signal
  - $H_{\text{cm}}$  the tangential component of the applied magnetic field at  $M_{\max}$ .
- Typical behaviour of these parameters in stressed materials:
  - Low  $M_{\max}$  values are measured in materials under compressive stresses.
  - High  $M_{\max}$  values are measured in materials under tensile stresses.
- $H_{\text{cm}}$  values show the opposite effect:
  - High  $H_{\text{cm}}$  : compressive stresses
  - Low  $H_{\text{cm}}$  : tensile stresses

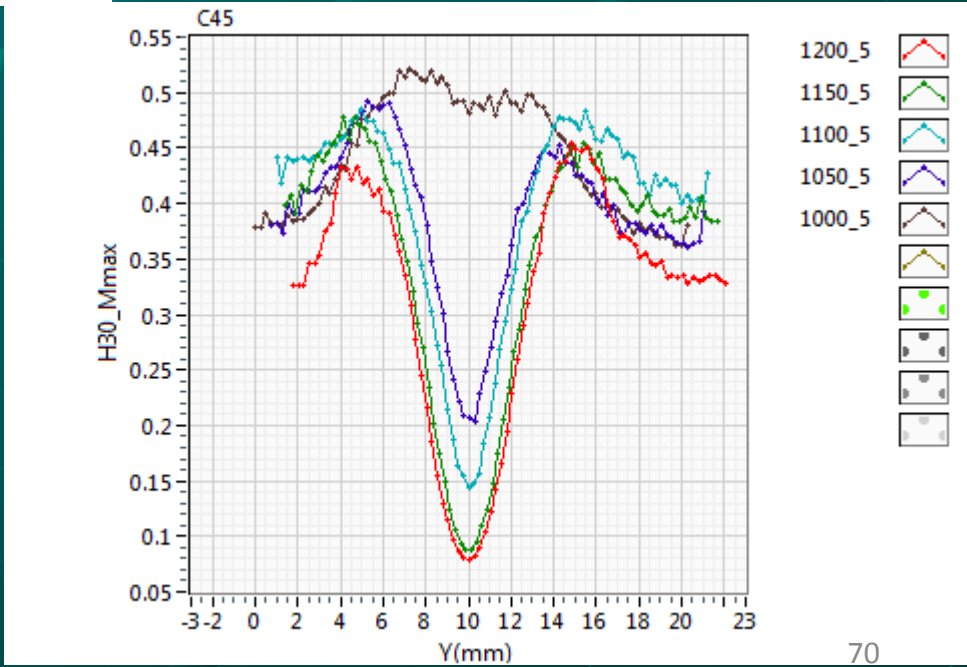
# C45 steel samples

Maximum amplitude of Barkhausen noise  $M_{max}$  [V] vs position on the sample.  $T_{treat}$  in [°C],  $v$  in [dm/min].



$v_{treat} = 3$  dm/min

$v_{treat} = 5$  dm/min



# Conclusions

- The localized hardening in the laser treated steel samples is the consequence of phase transformations: austenization followed by self-quenching.
- The phases are proeutectoid ferrite and pearlite or bainite in the base material, martensite and small amounts of retained austenite in the LHZ, a mixture of ferrite and martensite in the HAZ.
- By X-ray diffraction, tensile residual stresses were determined in the HAZ and compressive residual stresses in the LHZ and the BM.
- The positions of the HAZ and the LHZ were clearly detected in the micromagnetic experiments with 3MA-II.
- Moreover, in the C45 steels, samples treated at different temperatures and speeds could be classified.
- Point-probe experiments: apparently P7 is more sensitive than dt to the material properties under study
- Good agreement is observed among the results from the different techniques studied here.

# Acknowledgements

- Thanks are due to my colleagues, who participated in the works presented here.
- Thanks are due to CNEA, to MINCyT, to IAEA, to IZFP, to NIRDTP who financed much of the work presented here.
- Thanks are due to Prof. Nardoni and Dr. Dobmann, who invited me to NDT Academy.

# Some references

- Characterization of Cold Rolling-Induced Martensite in Austenitic Stainless Steels, M. Ruch, J. Fava, C. Spinosa, M. Landau, G. Cosarinsky, A. Savin, F. Novy, V. Turchenko, M. Craus. Accepted for 19 WCNDT, Munich, Germany, June 2016. <http://papers.dgzfp.de>.
- "Material characterization by electrical conductivity assessment using impedance analysis", Guillermo Cosarinsky, Javier Fava, Marta Ruch, Adrián Bonomi, Procedia Materials Science 9 (2015) 156–162; doi: 10.1016/j.mspro.2015.04.020; ISSN 2211- 8128
- "Non-Destructive Characterization of Laser Hardened Steels", G. Cosarinsky, M. Kopp, M. Rabung, G. Seiler, A. Petragalli, D. Vega, M. Sheikh-Amiri, M. Ruch, C. Boller, Insight 56(10), October 2014, 553-559; DOI 10.1784/insi.2014.56.10.553, ISSN 1354-2575
- "Automatic eddy current classification of signals delivered by flaws – application to nuclear fuel cladding", G. Cosarinsky, M. Ruch, G. Ruggirello, G. Domizzi, R. Grimberg, R. Steigmann, A. Savin, Insight 54(6), June 2012, 316-321; DOI 10.1784/insi.2012.54.6.316, ISSN 1354-2575
- "Calculation and simulation of impedance diagrams of planar rectangular spiral coils for eddy current testing", J. Fava, M. Ruch, NDT&E Int. 39(5), 2006, 414-424. ISSN 0963 8695
- "Comments on the stability of hydride phases in Zircaloy", L. Lanzani, M. Ruch. J. Nucl. Mater. 324, 2004, 165-176. ISSN: 0022-3115
- "Preparation of calibration standards for eddy-current assessment of non-conductive coating thickness", A. Perotti, L. Lanzani, P. Coronel, M. Ruch, Insight 43(5), 2001, 323-329.
- "Non-destructive assessment of the thickness of oxide layers on Zircaloy-4: influence of hydrogen content", A. Perotti, L. Lanzani, J.A. Marengo, M.Ruch, Insight 42(9), 2000, 597-602
- "Pressure Tubes Blister Detection by NDT", C. Belinco, G. Domizzi, A. García, M. Ruch, C. Desimone, J. Fava, IV PANNDT, IV Conferencia Panamericana de END, Buenos Aires, 22 al 26 de octubre 2007, ISBN 978-987-23957-0-4